AWARD NUMBER: W81XWH-14-1-0107

TITLE: Tumor Microenvironment Gene Signature as a Prognostic Classifier and Therapeutic Target

PRINCIPAL INVESTIGATOR: Sandra Orsulic, PhD

CONTRACTING ORGANIZATION: Cedars-Sinai Medical Center
Los Angeles, CA 90048

REPORT DATE: June 2015

TYPE OF REPORT: Annual

PREPARED FOR: U.S. Army Medical Research and Materiel Command
Fort Detrick, Maryland 21702-5012

REPORT DOCUMENTATION PAGE

Form Approved
OMB No. 0704-0188

1. REPORT DATE	2. REPORT TYPE	3. DATES COVERED
June 2015	Annual	05-05-2014 – 05-04-2015

4. TITLE AND SUBTITLE
Tumor Microenvironment Gene Signature as a

Prognostic Classifier and Therapeutic Target

5a. CONTRACT NUMBER
W81XWH-14-1-0107

5b. GRANT NUMBER

5c. PROGRAM ELEMENT NUMBER

6. AUTHOR(S)
Sandra Orsulic

E-Mail: orsulics@cshs.org

5d. PROJECT NUMBER

5e. TASK NUMBER

5f. WORK UNIT NUMBER

7. PERFORMING ORGANIZATION NAME(S) AND ADDRESS(ES)
Cedars-Sinai Medical Center
8700 Beverly Boulevard
Los Angeles, CA 90048

8. PERFORMING ORGANIZATION REPORT NUMBER

9. SPONSORING / MONITORING AGENCY NAME(S) AND ADDRESS(ES)

U.S. Army Medical Research and Materiel Command
Fort Detrick, Maryland 21702-5012

10. SPONSOR/MONITOR'S ACRONYM(S)

11. SPONSOR/MONITOR'S REPORT NUMBER(S)

12. DISTRIBUTION / AVAILABILITY STATEMENT

Approved for Public Release; Distribution Unlimited

13. SUPPLEMENTARY NOTES

14. ABSTRACT
Outcome predictors based on gene signatures have been successfully applied in breast cancer but similar predictors have not been developed for ovarian cancer. We identified a tumor microenvironment-based gene signature that correlates with poor survival in ovarian cancer patients. We are refining this gene signature to develop biomarkers for the identification of patients with adverse outcomes on standard treatment. In the first part of this project, we have analyzed a gene signature for the identification of patients who are unlikely to benefit from standard surgery and/or chemotherapy and should be considered for clinical trials targeting specific pathways in the tumor microenvironment. Specifically, we found that suboptimal surgical outcome is associated with a molecularly aggressive subtype of ovarian cancer characterized by the presence of reactive tumor stroma, which likely contributes to chemotherapy resistance. In the second part of the project, we will validate the gene signature in patient samples and develop a preliminary quantitative assay for use in the clinical setting. A validated gene signature to identify patients with adverse outcomes has the potential to reduce both the human and financial costs of ineffective therapies and associated toxicities. This will facilitate more individualized treatment decisions and improve the quality of care for patients with ovarian cancer.

15. SUBJECT TERMS
Ovarian cancer, prediction models, gene network analysis, gene signature, prognosis, clinical outcome, residual disease after cytoreductive surgery, therapy resistance, recurrence, survival

16. SECURITY CLASSIFICATION OF:			17. LIMITATION OF ABSTRACT	18. NUMBER OF PAGES	19a. NAME OF RESPONSIBLE PERSON
a. REPORT	b. ABSTRACT	c. THIS PAGE			USAMRMC
Unclassified	Unclassified	Unclassified	Unclassified	28	19b. TELEPHONE NUMBER *(include area code)*

Table of Contents

Page

1. **INTRODUCTION:**

The majority of patients with advanced stage epithelial ovarian cancer (EOC) present with advanced stage disease, which is currently treated by cytoreductive surgery and chemotherapy. Approximately 10% of EOC patients cannot be successfully cytoreduced by surgery and 20% are intrinsically resistant to chemotherapy or develop chemoresistant disease within one year from initial treatment. Currently, ovarian cancer surveillance and subsequent therapies are implemented on a "watch-and-wait" basis because there are no reliable biomarkers to identify patients with adverse outcomes on standard treatment. To identify biomarkers that predict adverse outcome in patients, we studied the key processes involved in metastatic ovarian cancer progression, including changes in the tumor microenvironment. This led to the identification of a stromal/extracellular matrix gene signature that correlates with poor patient survival. In the first part of this project, we have identified and optimized gene signatures for the identification of patients who are unlikely to benefit from standard surgery and/or chemotherapy. In the second part of the project, we will validate the gene signatures in patient samples and develop a preliminary quantitative assay for use in the clinical setting. The development of a reliable test for the identification of high risk patients is not only crucial to improving their clinical management but also timely because of the emergence of personalized treatment strategies for ovarian cancer. A validated gene signature to identify patients with adverse outcomes has the potential to reduce both the human and financial costs of ineffective therapies and associated toxicities. Importantly, implementation of the predictive signature assay will provide opportunities to deliver targeted therapies directed at the underlying mechanism of the poor prognosis signature. This will facilitate more individualized treatment decisions and improve the quality of care for patients with EOC.

2. **KEYWORDS:** Ovarian cancer, prediction models, gene network analysis, gene signature, prognosis, clinical outcome, residual disease after cytoreductive surgery, therapy resistance, recurrence, survival.

3. **ACCOMPLISHMENTS:**

- **What were the major goals of the project?**

Specific Aim 1 (specified in proposal)	**Timeline**	**% Completed**
Major Task 1 **Identify gene signatures for the prediction of poor outcome**	**Months**	
Subtask 1 Select biologically relevant covariates and build a multivariate model for the analysis of 3 datasets (TCGA, n=403; GSE26712, n=185; and GSE51088, n=122; these are public datasets with de-identified patient information).	1-3	100%
Subtask 2 Analyze datasets individually and in combination; derive gene signatures using multiple statistical methods; correlate with overall survival, progression-free survival, residual disease and other outcomes	4-6	100%

Subtask 3 Identify small subsets of predictive genes and their interactions	7-8	100%
Milestone Achieved A gene signature consisting of 8-15 genes with high predictive power in all three datasets	8	100%
Major Task 2 **Optimize the gene signature for the prediction of poor outcome**		
Subtask 1 Assess the predictive accuracy of the gene signatures using independent datasets (GSE9891 and GSE3149; these are public datasets with de-identified patient information)	9-10	100%
Subtask 2 Generate a test qPCR set from frozen samples of patients with extreme outcomes (10 with <1 year survival and 10 with >7 year survival); validate by qPCR up to 30 prioritized genes that have extremely high predictive power in individual datasets but are not present in all 3 datasets	11-12	10%
Subtask 3 Validate gene signature accuracy using statistical methods	13-14	0%
Milestone Achieved An independently validated set of 8-15 genes with high predictive power	14	0%
Major Task 3 **Validate the gene signature for the prediction of poor outcome**		
Subtask 1 Identify and collect 200 primary ovarian cancer patient samples with annotated demographic, pathologic and clinical information and follow-up (all patient samples will be de-identified)	3-7	100%
Subtask 2 Cut and stain slides (1 H&E + 9 unstained sections); evaluate the suitability of each sample by pathologic examination of tumor sections and circle the area on the slide for RNA isolation	8-9	50%
Subtask 3 Isolate RNA from slides; perform quality control	9-12	50%
Subtask 4 Design the Nanostring assay for the quantification of the signature genes; perform quality control; collect data	13-15	0%
Subtask 5 Analyze data using statistical methods; correlate with overall survival, progression-free survival, residual disease status and other outcomes that could be used to improve clinical management of ovarian cancer patients	16-21	0%

Subtask 6 Validate the gene signature assay using statistical models and risk prediction models with known parameters	21-22	0%
Subtask 7 Submit a manuscript on the predictive power of the optimized gene signature using microarray data and Nanostring assay data and deposit RNA expression data into public repository (GEO) Plan an academic multi-center validation of the Nanostring signature assay as required prior to FDA validation	23-24	0%
Milestone Achieved Validated gene signature gene assay for the prediction of clinical outcome(s) using paraffin-embedded tumor tissues	*22*	0%

- **What was accomplished under these goals?**
  - **1) Major activities:**

We primarily focused on computational network gene analyses for the discovery and validation of gene sets that are associated with adverse outcomes in ovarian cancer.

  - **2) Specific objectives:**

Our objectives were to identify a gene set of ~30 genes that significantly correlates with poor survival in three independent microarray datasets and to further refine individual gene signatures of ~10 genes that are most strongly associated with adverse patient outcomes, such as residual disease after cytoreductive surgery and poor survival. Advanced EOC typically presents with metastatic tumor nodules spread throughout the peritoneum. Standard treatment for EOC is primary surgical cytoreduction followed by adjuvant platinum- and taxane-based chemotherapy. The goal of surgery is to achieve complete cytoreduction (R0) as it has been shown that macroscopically visible residual disease (RD) is associated with poor progression-free and overall survival (1, 2). In cases where R0 cannot be achieved due to difficulty in resecting tumors that have invaded vital organs, it is preferable to forego primary cytoreduction surgery and use neoadjuvant chemotherapy to reduce the tumor burden and increase the chances of achieving R0 by interval cytoreduction surgery. At present, there is no clinically-applicable biomarker that can predict suboptimal cytoreduction. Several preoperative biomarkers have been evaluated, including computed tomography and serum CA-125 (3-6), but did not achieve sufficient specificity and/or sensitivity to be used in clinical decision-making (7). Consequently, many patients are left with a significant amount of residual disease and are not benefiting from aggressive surgery yet must endure the negative aspects of surgery, such as extended recovery time and delayed initiation of chemotherapy.

The crucial question that remains unanswered is what leads to poor survival in suboptimally cytoreduced patients. Two different scenarios have been proposed. In the first scenario, the amount of residual tumor cells dictates the chemotherapeutic accessibility and rate of tumor outgrowth. In the second scenario, the intrinsic aggressive tumor biology that is responsible for the failure in surgical resection is also responsible for resistance to chemotherapy and

a higher rate of growth and invasion. If unresectable tumors are biologically different from resectable tumors, it is expected that they would have different molecular profiles. Two recent studies used expression profile data to identify signatures of suboptimal primary cytoreduction and RD (8, 9). Although the two studies used different datasets and parameters of cytoreduction, the resultant gene signatures largely overlap and represent common biological processes, such as extracellular matrix remodeling, invasion and angiogenesis (8, 9). These processes have been previously associated with ovarian cancer progression and metastasis, favoring the idea that the success of surgical cytoreduction is dictated by tumor biology. Here, we analyze the molecular pathways associated with RD to identify underlying biological processes that determine surgical outcome and therapeutic efficacy.

- **3) Significant findings or key outcomes:**

Identification of the RD network genes. The three largest gene expression datasets for ovarian cancer, TCGA, GSE26712 (10), and GSE9891 (11), were downloaded from the curatedOvarianData database in R (12). Cytoreduction status and survival data are available in all three datasets. All datasets in the database had been preprocessed and normalized at the gene level. We restricted our study to primary, late-stage, serous ovarian tumors with available information on cytoreduction status. Samples of low-stage, non-serous EOC, metastases, or other diseases, were excluded from our analysis. There are 468, 182, and 167 patients available with 136, 93, and 66 suboptimally cytoreduced patients in the TCGA, GSE26712, and GSE9891 datasets, respectively. The TCGA and GSE26712 datasets were used to identify the molecular signatures, while the GSE9891 dataset was used for validating the signatures and evaluating their predictive power.

Candidate gene signatures were identified based on both differentiated genes and differentiated network structures. We first compared expression levels between optimal and suboptimal cytoreduction in the TCGA and GSE26712 datasets separately using 2-sample t-tests. With a P value of 0.05, 1206 differential expressed (DE) genes from the TCGA data and 979 DE genes from the GSE26712 data were selected (**Fig. 1A**). Among the selected DE genes, there were 136 gene signatures common to both datasets **(Fig. 1A**). We then merged the two datasets and constructed a common and differential co-expression network with a sparse graphical model (13). The suboptimal cytoreduction associated differential network was created from high-order (partial) correlations conditioning on the common (background) correlations. Eleven genes in the differentiated network were chosen as the candidate gene signatures, hereafter referred to as the RD network genes (**Fig. 1B**). All of the 11 RD network genes were validated in the independent GSE9891 dataset with low P values. Four RD network genes with the lowest P values are highlighted in red (**Fig. 2A**). The predictive power of the 11 RD network genes and the four RD network genes with the lowest P values was evaluated with logistic regression and predicted Area Under the ROC Curve (AUC) (**Fig. 2B**). In addition to categorizing patients into R0 and RD, the TCGA and GSE9891 datasets stratify patients by the amount of residual disease as follows: 0 mm, 1-10 mm, 11-20 mm, and >20 mm. For each of the four RD network genes with the lowest P values, we tested whether their levels increased with the increased amount of residual disease the TCGA and GSE9891 datasets. For most of the genes, expression levels were directly proportional to the amount of residual disease in both datasets (**Fig. 3**).

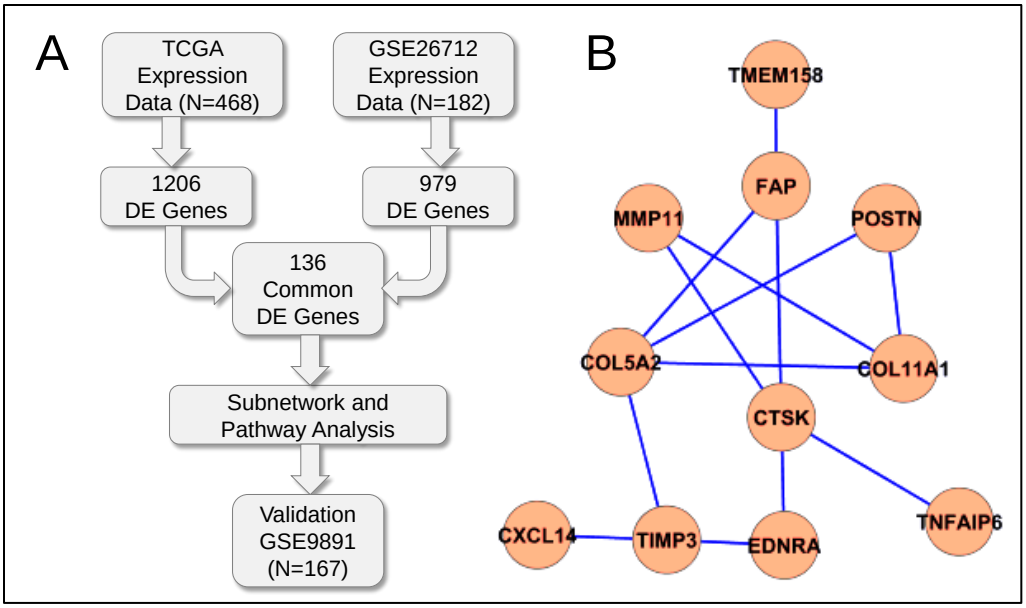

Fig. 1. Derivation and validation of the RD gene network. (A) Statistical analysis workflow chart. Normalized expression profile data from two datasets were screened for differentially expressed (DE) genes between patients with residual disease (RD) and patients without residual disease (R0) (TCGA dataset) or between patients with suboptimally and optimally cytoreduced tumors (GSE26712), $P < 0.05$. Common DE genes were used to build networks and pathways. **(B)** Selected biomarkers with both differentially expressed genes and differentiated networks.

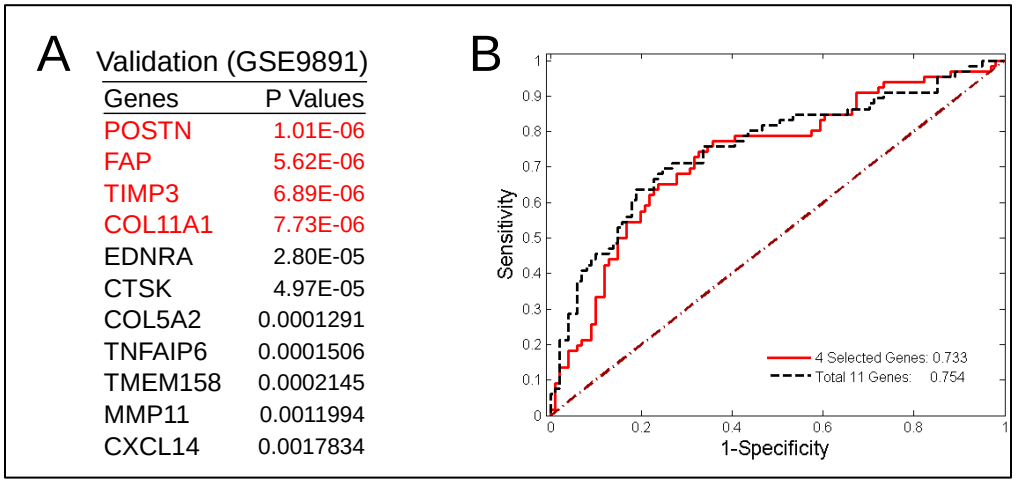

Fig. 2. Validation and predictive power of the RD gene network. (A) External validation of the network genes in the third dataset (GSE9891). Top four genes with the lowest P values are highlighted in red. **(B)** Predicted Area under the ROC Curve (AUC) for the RD network genes in the validation dataset.

Fig. 3 Expression levels of the RD network genes correlate with the amount of RD. Expression levels of the four RD network genes with the lowest P values are plotted according to the amount of residual disease in the TCGA and GSE9891 datasets. The x axis shows non-transformed expression levels in the TCGA dataset and log2 expression levels in the GSE9891 dataset. The y axis shows samples grouped by the amount of residual disease. The number of samples in each group is indicated in parentheses.

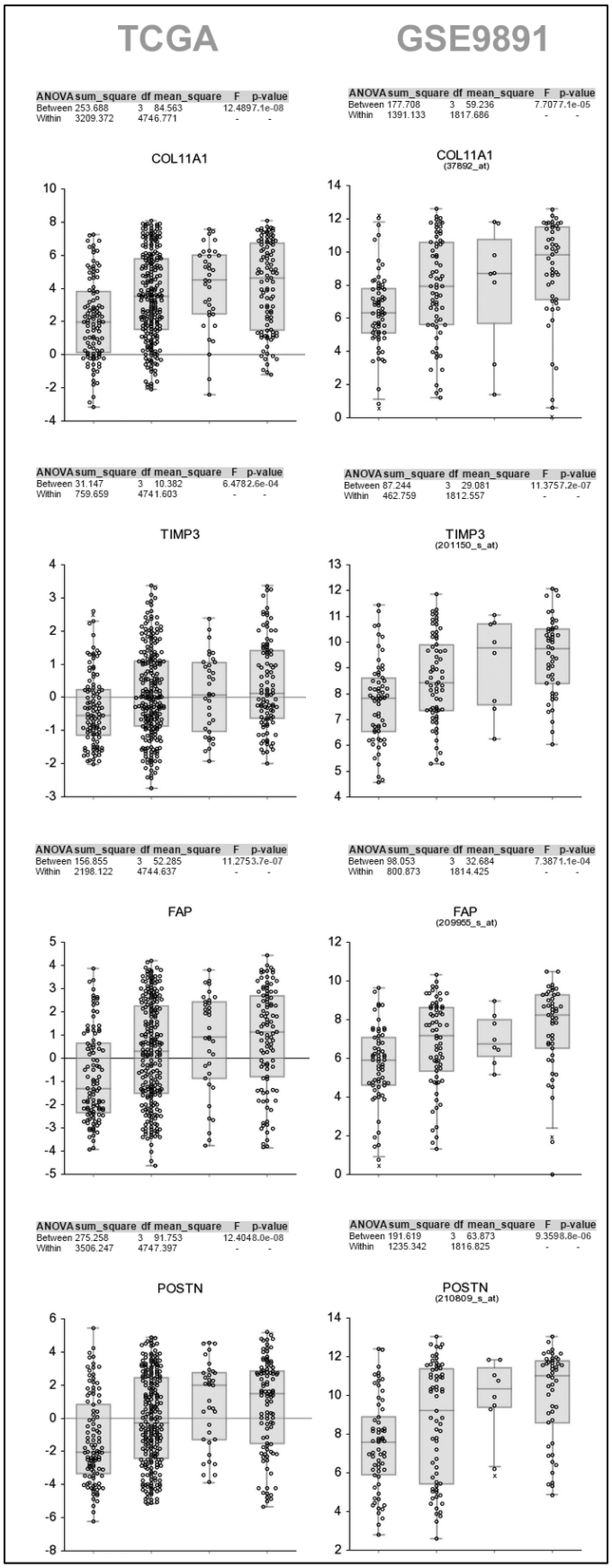

MOLECULAR SUBTYPE					
C1 (Desmoplastic)			Mesenchymal	
GSE9891			TCGA	
Tothill et al., 2008			Verhaak et al., 2013	
Code	Gene	FC	Gene	FC
UPREGULATED			UPREGULATED	
229479_at	LOC646324	10.845229	**POSTN**	17.7375
37892_at	**COL11A1**	12.750797	**COL11A1**	11.814
204320_at	**COL11A1**	11.48261	THBS2	8.69
223121_s_at	SFRP2	10.778471	**COL5A2**	8.1602
223122_s_at	SFRP2	11.445803	ASPN	7.954
229554_at	---	6.7281208	**FAP**	7.7823
226777_at	---	8.212894	MMP13	7.228
209955_s_at	**FAP**	7.1073287	VCAN	7.1822
229271_x_at	---	7.9877546	LUM	7.0656
218469_at	GREM1	9.4652992	COL10A1	6.9548
210511_s_at	INHBA	6.759526	**CTSK**	6.8514
227140_at	---	7.5750127	COMP	6.3478
1555778_a_at	**POSTN**	8.1021272	**CXCL14**	5.9748
206439_at	DSPC3	14.014552	FABP4	5.8968
227566_at	HNT	7.0989133	INHBA	5.6539
218468_s_at	GREM1	8.5588904	EPYC	5.5736
226311_at	---	5.6564597	DCN	5.3517
203083_at	THBS2	6.7203825	SFRP4	5.3411
219087_at	ASPN	5.3621277	GRP	5.2429
221729_at	**COL5A2**	5.2888374	COL1A1	5.1869
227061_at	---	6.5929295	CDH11	5.1591
217428_s_at	COL10A1	7.7148282	LRRC15	4.9104
221730_at	**COL5A2**	5.3857191	**MMP11**	4.8646
221541_at	CRISPLD2	5.8714302	COL3A1	4.7242
213909_at	LRRC15	7.0047274	COL5A1	4.5565
223278_at	GJB2	6.7386058	COL6A3	4.5497
215446_s_at	LOX	5.6062552	SERPINF1	4.4939
210809_s_at	**POSTN**	7.257405	VCAM1	4.4722
226997_at	---	5.199374	MMP2	4.459
213790_at	---	6.6941656	SULF1	4.3466
226695_at	PRRX1	5.4573365	AEBP1	4.2575
212488_at	COL5A1	5.4904627	PLAU	4.1823
212489_at	COL5A1	5.5601877	FBN1	4.1441
228481_at	**POSTN**	5.188377	SNAI2	4.1357
202952_s_at	ADAM12	5.4170294	COL1A2	4.0908
204619_s_at	CSPC2	5.2507707	FN1	4.0568
213338_at	RIS1	4.8451023	COLEC12	4.0038
235318_at	FBN1	4.2233672	TDO2	3.9742
235629_at	FN1	5.5047757	NNMT	3.8308
203878_s_at	**MMP11**	5.7548512	EDIL3	3.819
214702_at	FN1	5.2417849	CXCL12	3.7699
202766_s_at	FBN1	4.5106959	CRISPLD2	3.7449
202450_s_at	**CTSK**	4.7272828	FMO1	3.717
205941_s_at	COL10A1	5.3031691	ACTA2	3.7138
211571_s_at	CSPC2	4.8662663	GREM1	3.6798
202765_s_at	FBN1	4.3667779	ACTG2	3.5888
225242_s_at	CCDC80	4.9951303	CCL11	3.5874
215646_s_at	CSPC2	5.0022022	**TMEM158**	3.556
201150_s_at	**TIMP3**	4.8234097	**TIMP3**	3.527
226237_at	COL8A1	5.6902738	GLT8D2	3.5206
214587_at	COL8A1	4.768445	SPARC	3.4349
232805_at	**COL11A1**	5.3114646	HNT	3.4262
232458_at	COL3A1	5.3788569	ADAM12	3.4253
203325_s_at	COL5A1	4.2623934	C1QTNF3	3.3798
204464_s_at	**EDNRA**	3.8729738	SERPINE1	3.3452
204620_s_at	CSPC2	4.4118421	ITGBL1	3.3258
228367_at	ALPK2	4.0155324	LPPR4	3.3201
213125_at	OLFML2B	4.0182338	F13A1	3.2604
205991_s_at	PRRX1	4.1668024	**TNFAIP6**	3.1882
221731_x_at	CSPC2	4.4033451	LOX	3.1817
201852_x_at	COL3A1	3.8094741	ECM2	3.1546
212464_s_at	FN1	3.7758774	OMD	3.143
202311_s_at	COL1A1	4.3889329	MFAP5	3.1118
201792_at	AEBP1	3.8909698	COPZ2	3.1103
212667_at	SPARC	3.5960765	TAGLN	3.0986
227399_at	VGLL3	3.8108685	COL8A1	3.0604
216442_x_at	FN1	3.5597159	THBS1	3.0524
205700_at	HSD17B6	4.1587689	PCOLCE	3.0216
210495_x_at	FN1	3.5353473	COL16A1	3.0153
228396_at	---	3.1236609	TWIST1	3.0133
205479_s_at	PLAU	4.016159	PDLIM3	3.0065
238852_at	PRRX1	3.9321946	NT5E	2.9838
209621_s_at	PDLIM3	3.7308858	IL7R	2.9708
204589_at	NUAK1	3.481439	PRRX1	2.9703
211668_s_at	PLAU	4.210605	CDR1	2.9407
205713_s_at	COMP	4.0295213	FGF7	2.9378
243864_at	CCDC80	3.3953216	PTGIS	2.9297
203876_s_at	**MMP11**	5.7806191	SRPX	2.9186
205422_s_at	ITGBL1	4.8460929	TGFBI	2.9087
206026_s_at	**TNFAIP6**	3.4272275	OLFML2B	2.9054
213247_at	SVEP1	3.6569271	SCG2	2.8918
211719_x_at	FN1	3.4190114	CILP	2.8758
206025_s_at	**TNFAIP6**	3.4059246	CALB2	2.8742
225681_at	CTHRC1	4.0173589	NID2	2.8565
37512_at	HSD17B6	3.7896423	ECM1	2.8458
219655_at	C7orf10	4.132224	COL6A2	2.832
202310_s_at	COL1A1	3.697839	HEPH	2.7959
235182_at	C20orf82	2.2309295	PITX2	2.785
205100_at	GFPT2	2.89878	ADAMTS12	2.7705
201744_s_at	LUM	4.1098657	RAB31	2.7698
226834_at	---	3.6172112	ALDH1A3	2.751
219529_at	CLIC3	2.1528261	MOXD1	2.7504
207134_x_at	TPSAB1	2.0642319	SEMA3D	2.7442
218730_s_at	OGN	2.2783526	GPNMB	2.7386
1559280_a_at	---	2.0039755	ADRA2A	2.722
226535_at	---	2.2083261	LAMB1	2.7121
209763_at	CHRDL1	2.3325837	NUAK1	2.7108
204563_at	SELL	2.0008696	BGN	2.7071
202827_s_at	MMP14	2.127053	PDPN	2.693
206157_at	PTX3	2.0716112	DPT	2.6677

The RD gene network is enriched in aggressive molecular subtypes of ovarian cancer. We then set out to determine whether the RD network genes were associated with any previously identified molecular subtypes of EOC. Two comprehensive studies have identified several distinct molecular subtypes of EOC based on expression profiles (11, 14). In the study by Tothill et al., 251 EOC samples clustered into six molecular subtypes (C1-C6), of which the C1 (mesenchymal) subtype correlated with extensive desmoplasia and dismal prognosis (11). In the study by Verhaak et al., 489 high grade serous EOCs from the TCGA dataset clustered into four molecular subtypes (differentiated, immunoreactive, mesenchymal, and proliferative) (14), of which the mesenchymal subtype had the worst survival (15, 16). These molecular subtypes suggest associations between poor survival and specific biological features, such as mesenchymal cell state and desmoplasia. In order to identify if the 11 RD network genes were enriched in any of the identified molecular subtypes of EOC, we searched for the presence of the genes in the top 100 probes specifically upregulated in the C1-C6 subtypes as well as in the top 100 genes specifically upregulated in the differentiated, immunoreactive, mesenchymal, and proliferative molecular subtypes. This analysis revealed that the RD network genes were highly enriched in the C1 and mesenchymal molecular subtypes of EOC (data not shown). Nine of 11 RD network genes were present in the top 100 probes upregulated in the C1 subtype and 10 of 11 RD network genes were present in the top 100 genes upregulated in the mesenchymal subtype (**Table 1**). This result strongly suggests that the RD gene network largely represents samples characterized by the C1/mesenchymal molecular subtype.

Table 1. The RD network genes are highly enriched in the desmoplastic/mesenchymal molecular subtype of primary EOC. Shown are the top 100 upregulated probes that are differentially expressed in the C1 (desmoplastic) subtype in the Tothill (GSE9891) dataset and the top 100 upregulated genes that are differentially expressed in the mesenchymal subtype in the TCGA dataset. The top 100 upregulated probes/genes were arbitrarily selected as a cut-off point. RD network genes are indicated in red.

OMENTAL METASTASIS

17 Omental Mets vs 13 Primary		
PMID: 17346539		
Bignotti et al., 2007		
Code	Gene	FC
UPREGULATED		
204320_at	**COL11A1**	8.23
37892_at	**COL11A1**	6.33
217430_x_at	COL1A1	5.67
201150_s_at	**TIMP3**	5.52
201149_s_at	**TIMP3**	5.46
214701_s_at	FN1	5.4
210511_s_at	INHBA	4.94
201842_s_at	EFEMP1	4.86
206439_at	DSPG3	4.36
221730_at	**COL5A2**	4.07
215446_s_at	LOX	4.03
201147_s_at	**TIMP3**	4.01
213764_s_at	MFAP5	4.01
210809_s_at	**POSTN**	3.97
203325_s_at	COL5A1	3.95
203083_at	THBS2	3.91
202766_s_at	FBN1	3.9
209955_s_at	**FAP**	3.84
212488_at	COL5A1	3.82
214336_s_at	COPA	3.81
209621_s_at	PDLIM3	3.75
211571_s_at	CSPG2	3.74
212489_at	COL5A1	3.73
214587_at	COL8A1	3.7
213338_at	RIS1	3.44
203876_s_at	**MMP11**	3.37
201843_s_at	EFEMP1	3.28
209541_at	IGF1	3.26
212464_s_at	FN1	3.23
220988_s_at	NA	3.23
206658_at	UPK3B	3.2
201262_s_at	BGN	3.16
221729_at	**COL5A2**	3.15
202311_s_at	COL1A1	3.12
209754_s_at	TMPO	3.11
203878_s_at	**MMP11**	3.08
215646_s_at	CSPG2	3.07
202238_s_at	NNMT	3.05
211668_s_at	PLAU	3.02
216442_x_at	FN1	3.02
209754_s_at	TMPO	3.11
203878_s_at	**MMP11**	3.08
215646_s_at	CSPG2	3.07
202238_s_at	NNMT	3.05
211668_s_at	PLAU	3.02
216442_x_at	FN1	3.02
213765_at	MFAP5	3
204989_s_at	ITGB4	2.99
212344_at	SULF1	2.98
201108_s_at	THBS1	2.94
204619_s_at	CSPG2	2.94
202237_at	NNMT	2.91
217428_s_at	COL10A1	2.9
201852_x_at	COL3A1	2.89
201559_s_at	CLIC4	2.85
212952_at	CALR	2.82
204298_s_at	LOX	2.8
206002_at	GPR64	2.79
210892_s_at	GTF2I	2.79
202274_at	ACTG2	2.78
205428_s_at	CALB2	2.77
204589_at	ARK5	2.75
206227_at	CILP	2.73
201109_s_at	THBS1	2.72
207173_x_at	CDH11	2.69
205907_s_at	OMD	2.66
210495_x_at	FN1	2.66
204620_s_at	CSPG2	2.65
212354_at	SULF1	2.65
200974_at	ACTA2	2.64
201792_at	AEBP1	2.64
205941_s_at	COL10A1	2.63
215076_s_at	COL3A1	2.63
201744_s_at	LUM	2.58
202310_s_at	COL1A1	2.58
221541_at	CRISPLD2	2.58
205991_s_at	PRRX1	2.56
211719_x_at	FN1	2.55
202998_s_at	LOXL2	2.5
221731_x_at	CSPG2	2.5
205018_s_at	MBNL2	2.46
212667_at	SPARC	2.46
209466_x_at	PTN	2.42
203939_at	NT5E	2.41
202450_s_at	**CTSK**	2.4
203868_s_at	VCAM1	2.39
211161_s_at	COL3A1	2.37
213139_at	SNAI2	2.37
213496_at	LPPR4	2.34
208879_x_at	C20orf14	2.33
212105_s_at	DHX9	2.33
201438_at	COL6A3	2.32
213125_at	OLFML2B	2.32
212353_at	SULF1	2.3
207172_s_at	CDH11	2.29
202388_at	RGS2	2.28
201110_s_at	THBS1	2.27
210139_s_at	PMP22	2.27
213548_s_at	H41	2.26
205547_s_at	TAGLN	2.25

96 Omental Mets vs 198 Primary		
GSE2109 (GEO2R analysis)		
Expression Project for Oncology		
ID	Gene	logFC
UPREGULATED		
223121_s_at	SFRP2	4.466
223122_s_at	SFRP2	4.044
203980_at	FABP4	3.522
209613_s_at	ADH1B	3.113
206439_at	EPYC	3.05
210809_s_at	**POSTN**	2.971
204320_at	**COL11A1**	2.943
37892_at	**COL11A1**	2.854
205913_at	PLIN1	2.813
1555778_a_at	**POSTN**	2.797
209612_s_at	ADH1B	2.699
240135_x_at		2.492
213764_s_at	MFAP5	2.386
227061_at	LOC100506621	2.21
207175_at	ADIPOQ	2.16
206201_s_at	MEOX2	2.15
219087_at	ASPN	2.125
205433_at	BCHE	2.07
213247_at	SVEP1	2.04
201744_s_at	LUM	2.04
218469_at	GREM1	2.039
226237_at	COL8A1	2.01
235978_at	FABP4	2.01
229271_x_at	**COL11A1**	1.962
212713_at	MFAP4	1.94
201150_s_at	**TIMP3**	1.915
229479_at		1.892
224396_s_at	ASPN	1.885
213068_at	DPT	1.883
218468_s_at	GREM1	1.867
205713_s_at	COMP	1.847
212353_at	SULF1	1.831
213765_at	MFAP5	1.822
203886_s_at	FBLN2	1.815
212344_at	SULF1	1.796
226311_at	ADAMTS2	1.796
225242_s_at	CCDC80	1.785
215214_at	IGL	1.762
228766_at	CD36	1.76
228481_at		1.757
206488_s_at	CD36	1.723
217428_s_at	COL10A1	1.713
210511_s_at	INHBA	1.708
228186_s_at	RSPO3	1.707
201147_s_at	**TIMP3**	1.686
225241_at	CCDC80	1.685
209763_at	CHRDL1	1.684
205422_s_at	ITGBL1	1.673
236738_at	C3orf80	1.672
202238_s_at	NNMT	1.615
209955_s_at	**FAP**	1.613
227140_at	INHBA	1.61
207977_s_at	DPT	1.608
202994_s_at	FBLN1	1.607
229554_at		1.595
215446_s_at	LOX	1.591
229476_s_at	THRSP	1.587
231993_at	ITGBL1	1.586
228409_at	PLIN4	1.579
209614_at	ADH1B	1.578
212354_at	SULF1	1.574
202628_s_at	SERPINE1	1.568
219523_s_at	TENM3	1.564
201149_s_at	**TIMP3**	1.563
215646_s_at	VCAN	1.563
227566_at	NTM	1.551
209555_s_at	CD36	1.544
211571_s_at	VCAN	1.533
221541_at	CRISPLD2	1.53
1568765_at	SERPINE1	1.525
209758_s_at	MFAP5	1.523
221730_at	**COL5A2**	1.52
203083_at	THBS2	1.513
203548_s_at	LPL	1.51
221729_at	**COL5A2**	1.507
228367_at	ALPK2	1.5
205907_s_at	OMD	1.488
226695_at	PRRX1	1.482
201148_s_at	**TIMP3**	1.481
208335_s_at	DARC	1.478
227419_x_at	PLAC9	1.475
203876_s_at	**MMP11**	1.466
202237_at	NNMT	1.465
226777_at	ADAM12	1.457
209687_at	CXCL12	1.443
236044_at	PPAPDC1A	1.439
202765_s_at	FBN1	1.426
204457_s_at	GAS1	1.423
205941_s_at	COL10A1	1.388
219655_at	C7orf10	1.377
213909_at	LRRC15	1.371
225681_at	CTHRC1	1.366
204619_s_at	VCAN	1.361
206666_at	GZMK	1.349
221731_x_at	VCAN	1.342
205117_at	FGF1	1.34
210072_at	CCL19	1.339
203666_at	CXCL12	1.333
225664_at	COL12A1	1.328
202450_s_at	**CTSK**	1.326

Matched 9 Omental Mets vs 9 Primary		
GSE30587 (GEO2R analysis)		
Brodsky et al., 2014		
ID	Gene	logFC
UPREGULATED		
8151532	FABP4	2.523
8103254	SFRP2	2.26
7965390	EPYC	2.089
8056257	**FAP**	1.825
8106743	VCAN	1.79
7918064	**COL11A1**	1.789
8139207	INHBA	1.737
8134263	COL1A2	1.666
8046922	COL3A1	1.549
8170648	BGN	1.532
8059905	COL6A3	1.523
7919815	**CTSK**	1.513
8075635	**TIMP3**	1.494
7934906	ACTA2	1.474
8130867	THBS2	1.47
7969861	ITGBL1	1.463
7982597	THBS1	1.429
8016646	COL1A1	1.417
8058765	FN1	1.403
8132557	AEBP1	1.389
7995681	MMP2	1.368
7943998	NNMT	1.348
8057620	**COL5A2**	1.263
8081235	COL8A1	1.254
8003667	SERPINF1	1.25
8171172	MXRA5	1.193
7936968	ADAM12	1.17
7907222	PRRX1	1.168
8072626	**TIMP3**	1.165
7944082	PCSK7	1.156
8098441	TENM3	1.122
8113709	LOX	1.119
8129573	MOXD1	1.117
8143772	RARRES2	1.112
7989985	ITGA11	1.08
8123104	FNDC1	1.074
8035517	COMP	1.056
8024111	CNN2	1.052
8138289	ETV1	1.039
7997642	CRISPLD2	1.032
7952268	THY1	1.021
8072876	LGALS1	1.002
8104901	IL7R	0.974
8018761	ST6GALNAC2	0.965
7902495	NEXN	0.955
8067839	KGFLP1	0.952
7921882	OLFML2B	0.94
8042439	ANTXR1	0.92
7928429	PLAU	0.914
7973336	MMP14	0.896
8048749	KCNE4	0.845
8084710	ADIPOQ	0.842
7945245	NTM	0.837
8114920	DPYSL3	0.832
7970441	GJB2	0.818
8075728	MYH9	0.798
8142194	LAMB1	0.786
7956301	LRP1	0.781
8155487	KLF2	0.776
8161423	KLF2	0.776
8161455	KLF2	0.776
8077441	BHLHE40	0.773
8144917	LPL	0.762
7980152	LTBP2	0.761
8108217	TGFBI	0.76
8148572	LY6E	0.758
8148448	KHDRBS3	0.754
8076455	RRP7B	0.737
8069269	COL6A1	0.724
8024485	GADD45B	0.722
8159142	COL5A1	0.706
8086125	TRANK1	0.703
8175039	ELF4	0.682
7966026	NUAK1	0.681
7982377	GREM1	0.676
8026139	NFIX	0.668
8027778	FXYD5	0.663
8038683	KLK6	0.66
8010287	C1QTNF1	0.647
8021946	COLEC12	0.642
8067233	PMEPA1	0.641
8151684		0.64
7902452	AK5	0.625
8111387	ADAMTS12	0.625
8120043	RUNX2	0.62
8073775	FBLN1	0.618
8004510	CD68	0.618
7956856	MSRB3	0.617
7992789	TNFRSF12A	0.614
8015387	KRT17	0.61
7986446	ALDH1A3	0.599
8023995	FSTL3	0.597
8149774	LOXL2	0.585
7946589	MRVI1	0.582
8030128	PPP1R15A	0.575
7964119	STAT2	0.572
8129082	COL10A1	0.563
8029006	AXL	0.55
8041048	FOSL2	0.55
8024246	C19orf24	0.548

The RD gene network is enriched in metastatic ovarian cancer. We previously identified three of the four top-scoring RD network genes (POSTN, TIMP3, and COL11A1) as part of a 10-gene signature of poor survival in EOC and observed that these genes were upregulated in metastatic EOC in comparison to primary EOC (17, 18). To identify gene signatures associated with metastasis, we compared expression profiles of omental EOC metastases to primary EOC using three microarray datasets: Bignotti et al. (17 metastases, 13 primary EOC); GSE2109 (96 metastasis, 198 primary EOC); and GSE30587 (matched omental metastases and primary EOC from nine patients (19)). The RD network genes were highly enriched in the signatures of omental metastasis, with five of 11 RD network genes (FAP, TIMP3, COL11A1, CTSK, and COL5A2) present in all three metastasis signatures (**Table 2**). The striking similarity of the RD gene signature to the signatures of EOC metastasis indicates that ineffective primary cytoreduction may be related to the invasive nature of EOC.

Table 2. The RD network genes are highly enriched in omental metastases. Shown are the top 100 upregulated probes/genes that are differentially expressed in each of the three datasets comparing expression profiles of omental metastases to primary EOC. The top 100 upregulated probes/genes were arbitrarily selected as a cut-off point. RD network genes are indicated in red.

Tumor stroma, rather than malignant cells, is responsible for expression of the RD network genes. Gene Set Enrichment Analysis (GSEA) was used for annotation of the 11 RD network genes into hallmark genes (H) and GO Gene Sets (C5). The most significant hallmark associated with the expression of the RD network genes was epithelial-mesenchymal transition (EMT) in wound healing, fibrosis and metastasis, while extracellular matrix (ECM) was identified as the most likely site of protein expression (data not shown). Both malignant epithelial cells and supporting stromal cells secrete ECM in tumors making it difficult to identify the exact source of ECM proteins. We have previously shown by tumor *in situ* hybridization that one of the RD network genes, COL11A1, is primarily expressed in stromal cells and that the amount of stromal cells expressing COL11A1 increases during ovarian cancer progression in patient-matched primary, metastatic, and recurrent tumors (18). Other studies have shown that several of the RD network genes, including POSTN, TIMP3, and COL11A1, are enriched in the stromal rather than epithelial tumor component during EOC progression, with the highest levels identified in recurrent tumors (20). The increase in RD network gene expression in metastatic and recurrent tumors could be a reflection of an increased percentage of stromal cells and decreased percentage of malignant tumor cells. To test this hypothesis, we compared the levels of the RD network genes with the stromal marker, VIM, and the epithelial marker, EPCAM, in nine patient-matched metastatic and primary tumors in the GSE30587 dataset. Although metastatic tumors in comparison to primary tumors showed an increase in VIM and a decrease in EPCAM levels, these changes were modest in comparison to the differential expression of most RD network genes (**Fig. 4**). Similar results were obtained in additional datasets comparing metastatic and primary tumors (data not shown). Thus, an increase in RD network gene expression in metastatic tumors cannot be solely explained by an increased ratio of stromal to epithelial cells.

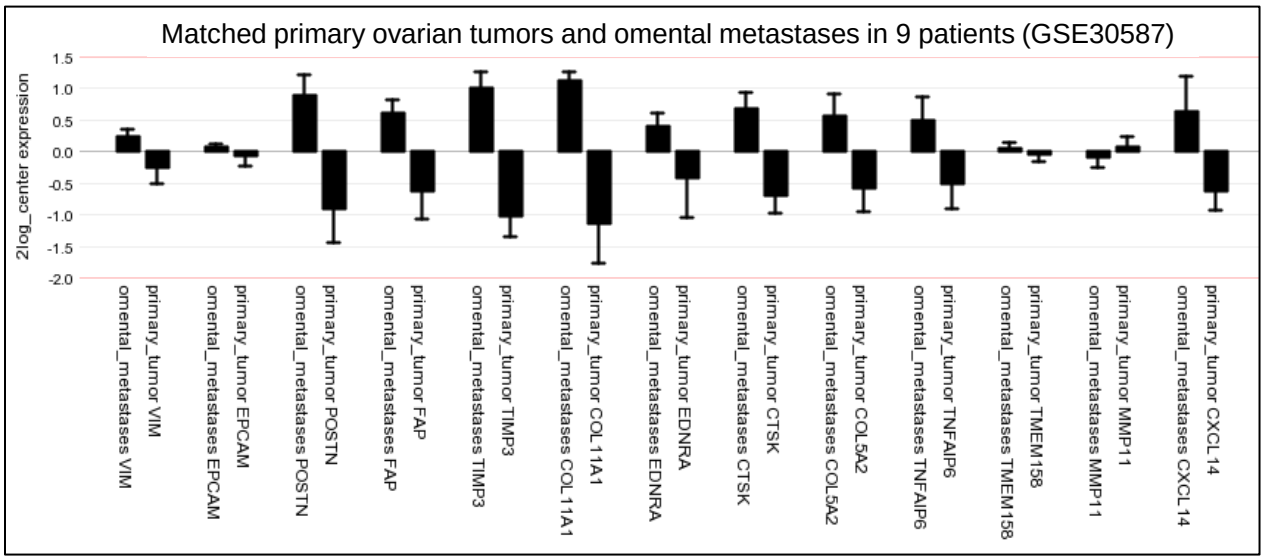

Fig. 4. Increased expression of most of the RD network genes in metastatic tumors is not a reflection of increased stromal to epithelial ratio. Relative expression levels of stromal (VIM) and epithelial (EPCAM) markers and in the 11 RD network genes in patient-matched EOC omental metastases and primary tumors.

The increase in RD network gene expression during cancer progression could be a reflection of a qualitative change in tumor stroma. The progression of epithelial tumors is known to be associated with desmoplasia or the increased presence of 'reactive stroma' (21). Reactive stroma is characterized by de novo production of α-smooth muscle actin (α-SMA) and increased remodeling of ECM components (22). FAP, one of the RD network genes, is typically used as a marker of reactive stroma in cancer (21). Next, we evaluated expression of the RD network genes in different ovarian tissue components using publically-available gene expression profiles in the GSE40595 dataset,in which the following tissues were laser-microdissected: 1) stroma from normal ovary, 2) stroma from ovarian cancer, 3) ovarian surface epithelium from normal ovary, and 3) epithelium from ovarian cancer (23). The results showed that the RD network genes were primarily expressed in the cancer stroma (**Fig. 5**).

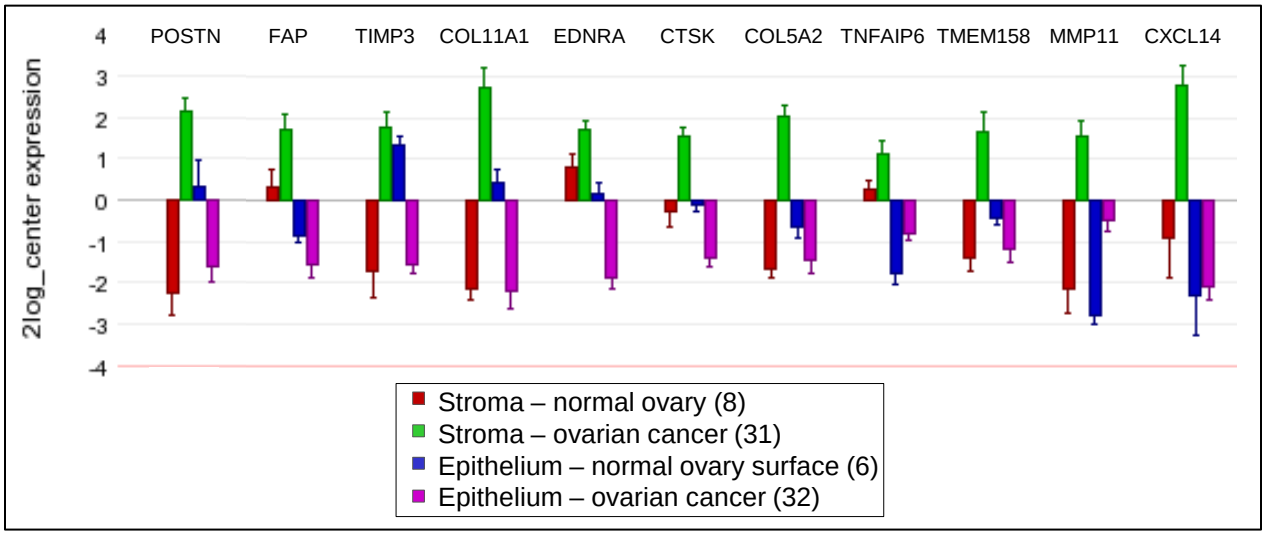

Fig. 5. Relative expression of the RD network genes in microdissected stromal and epithelial components in the normal ovary and ovarian cancer. The RD network genes are primarily expressed in the cancer-associated stroma.

Conclusions

Suboptimal primary cytoreductive surgery in advanced epithelial ovarian cancer (EOC) is associated with poor survival but it is unknown if this is due to the intrinsic biology of unresectable tumors. Currently, there are no clinically useful predictive models for surgical success, highlighting the need to understand the role of tumor biology in surgical outcome. Our objective was to identify the potential biological pathway(s) and cell type(s) that may be responsible for suoptimal surgical resection. Significant progress has been made in associating tumor biology with different molecular subtypes of EOC (11, 14). If tumor biology determines surgical success, it should be possible to link molecular subtypes of EOC with surgical outcome. Indeed, Tothill et al. observed in their study that the majority of patients with the C1 subtype had extensive RD (11). Our study shows that the molecular pathways associated with RD are highly enriched in the C1/mesenchymal molecular subtype of EOC. Additionally, we show that the RD gene network is enriched in metastatic and recurrent tumors, indicating that the

C1/mesenchymal subtype of EOC has characteristics of progressed EOC, however, we cannot exclude the possibility that the C1/mesenchymal subtype tumors are actually self-metastases rather than primary tumors.

Expression profile data are typically obtained from tumor specimens that contain various types and amounts of stromal cells, making it difficult to discern which cell types contribute to specific signatures. Our gene set enrichment analysis pointed to EMT as the most significant hallmark associated with the RD network genes. Studies in cancer and fibrosis have demonstrated that epithelial cells can generate tumor stroma through EMT (24, 25). However, two recent studies in colorectal carcinoma showed that the EMT gene signature in colorectal cancer is derived from tumor-associated stroma rather than from malignant cells converting to a mesenchymal phenotype (26, 27). Isella et al. analyzed patient-derived xenograft (PDX) models in which epithelial tumor cells continue to proliferate when propagated in mice while non-proliferating stromal cells die out. Human- and mouse-specific RNA sequencing demonstrated that the human mesenchymal signature is decreased in PDXs in comparison to primary tumors, indicating that the EMT signature is derived from stromal tumor cells (26). Callon et al. used FACS to isolate epithelial cells and fibroblasts from primary tumors and showed that the mesenchymal signature was enriched in tumor fibroblasts (27). Thus, two studies implementing different techniques came to a similar conclusion that the EMT signature is derived from stromal cells. Consistent with these studies, we show that the RD gene network, which significantly overlaps with the EMT signature in colorectal cancer, is also derived from tumor stroma in EOC. The tumor microenvironment has been increasingly recognized as a major player in the pathogenesis of EOC (28, 29). Our data indicate that stromal activation may also impact surgical outcome.

Development of a biomarker assay for the detection of the RD gene network in a preoperative image-guided tumor biopsy may be useful in deciding whether patients should be treated with primary cytoreductive surgery or neoadjuvant chemotherapy. We anticipate that such an assay would identify patients who are unlikely to benefit from primary cytoreduction and spare them the ineffective and frequently morbid surgical procedure as well as facilitate timely initiation of neoadjuvant chemotherapy. Another application of the RD biomarker assay would be in selecting the appropriate chemotherapy. Three of the four RD network genes with lowest P values (POSTN, FAP, and TIMP3) were also identified as the top three upregulated genes associated with therapeutic resistance in EOC (20), suggesting that patients with unresectable disease may also be resistant to neoadjuvant chemotherapy. Additionally, five of 11 RD network genes (POSTN, FAP, CTSK, COL5A2, and MMP11) are present in the 50-gene signature of neoadjuvant chemotherapy-resistance in breast cancer, which was also shown to be associated with increased desmoplasia (30), indicating that the presence of reactive stroma may cause multidrug resistance or restrict chemotherapy access. Thus, it may be necessary to target the reactive tumor stroma before or concurrently with chemotherapy to achieve therapeutic success in patients with RD.

Development of agents that target tumor stroma will require a better understanding of the key regulators of stromal activation and the mechanisms by which the reactive stroma contributes to unsuccessful surgical resection, tumor progression, and chemotherapy resistance. A possible treatment strategy may come from outside of the cancer field as stromal activation in cancer has significant similarities to matrix remodeling in fibrosis, a process that has been extensively studied for targeted therapy. Although there are no Food and Drug Administration (FDA)-approved

treatments for organ fibrosis, a large number of compounds have shown promising results in reversing fibrosis in preclinical models and are being tested in human clinical trials for systemic fibrosis conditions (31). We envision that repurposing these agents for cancer treatment may be effective in reversing stromal activation in cancer and increasing the efficacy of cytoreductive surgery and chemotherapy.

References

1. Shih KK, Chi DS. Maximal cytoreductive effort in epithelial ovarian cancer surgery. J Gynecol Oncol. 2010;21:75-80.
2. Chang SJ, Bristow RE, Ryu HS. Impact of complete cytoreduction leaving no gross residual disease associated with radical cytoreductive surgical procedures on survival in advanced ovarian cancer. Ann Surg Oncol. 2012;19:4059-67.
3. Bristow RE, Tomacruz RS, Armstrong DK, Trimble EL, Montz FJ. Survival effect of maximal cytoreductive surgery for advanced ovarian carcinoma during the platinum era: a meta-analysis. J Clin Oncol. 2002;20:1248-59.
4. Ferrandina G, Sallustio G, Fagotti A, Vizzielli G, Paglia A, Cucci E, et al. Role of CT scan-based and clinical evaluation in the preoperative prediction of optimal cytoreduction in advanced ovarian cancer: a prospective trial. Br J Cancer. 2009;101:1066-73.
5. Chi DS, Zivanovic O, Palayekar MJ, Eisenhauer EL, Abu-Rustum NR, Sonoda Y, et al. A contemporary analysis of the ability of preoperative serum CA-125 to predict primary cytoreductive outcome in patients with advanced ovarian, tubal and peritoneal carcinoma. Gynecol Oncol. 2009;112:6-10.
6. Axtell AE, Lee MH, Bristow RE, Dowdy SC, Cliby WA, Raman S, et al. Multi-institutional reciprocal validation study of computed tomography predictors of suboptimal primary cytoreduction in patients with advanced ovarian cancer. J Clin Oncol. 2007;25:384-9.
7. Ibeanu OA, Bristow RE. Predicting the outcome of cytoreductive surgery for advanced ovarian cancer: a review. Int J Gynecol Cancer. 2010;20 Suppl 1:S1-11.
8. Tucker SL, Gharpure K, Herbrich SM, Unruh AK, Nick AM, Crane EK, et al. Molecular biomarkers of residual disease after surgical debulking of high-grade serous ovarian cancer. Clin Cancer Res. 2014;20:3280-8.
9. Riester M, Wei W, Waldron L, Culhane AC, Trippa L, Oliva E, et al. Risk prediction for late-stage ovarian cancer by meta-analysis of 1525 patient samples. J Natl Cancer Inst. 2014;106.
10. Bonome T, Levine DA, Shih J, Randonovich M, Pise-Masison CA, Bogomolniy F, et al. A gene signature predicting for survival in suboptimally debulked patients with ovarian cancer. Cancer Res. 2008;68:5478-86.
11. Tothill RW, Tinker AV, George J, Brown R, Fox SB, Lade S, et al. Novel molecular subtypes of serous and endometrioid ovarian cancer linked to clinical outcome. Clin Cancer Res. 2008;14:5198-208.
12. Ganzfried BF, Riester M, Haibe-Kains B, Risch T, Tyekucheva S, Jazic I, et al. curatedOvarianData: clinically annotated data for the ovarian cancer transcriptome. Database-the Journal of Biological Databases and Curation. 2013.
13. Liu Z, Sun F, Braun J, McGovern D, Piantadosi S. Multilevel Regularized Regression for Simultaneous Taxa Selection and Network Construction with Metagenomic Count Data. Bioinformatics. 2014.
14. Verhaak RG, Tamayo P, Yang JY, Hubbard D, Zhang H, Creighton CJ, et al. Prognostically relevant gene signatures of high-grade serous ovarian carcinoma. J Clin Invest. 2013;123:517-25.
15. Zhang W, Liu Y, Sun N, Wang D, Boyd-Kirkup J, Dou X, et al. Integrating genomic, epigenomic, and transcriptomic features reveals modular signatures underlying poor prognosis in ovarian cancer. Cell Rep. 2013;4:542-53.
16. Konecny GE, Wang C, Hamidi H, Winterhoff B, Kalli KR, Dering J, et al. Prognostic and therapeutic relevance of molecular subtypes in high-grade serous ovarian cancer. J Natl Cancer Inst. 2014;106.
17. Cheon DJ, Orsulic S. Ten-gene biomarker panel: a new hope for ovarian cancer? Biomark Med. 2014;8:523-6.

18. Cheon DJ, Tong Y, Sim MS, Dering J, Berel D, Cui X, et al. A collagen-remodeling gene signature regulated by TGF-beta signaling is associated with metastasis and poor survival in serous ovarian cancer. Clin Cancer Res. 2014;20:711-23.
19. Brodsky AS, Fischer A, Miller DH, Vang S, MacLaughlan S, Wu HT, et al. Expression profiling of primary and metastatic ovarian tumors reveals differences indicative of aggressive disease. PLoS One. 2014;9:e94476.
20. Ryner L, Guan Y, Firestein R, Xiao Y, Choi Y, Rabe C, et al. Up-Regulation of Periostin and Reactive Stroma is Associated with Primary Chemoresistance and Predicts Clinical Outcomes in Epithelial Ovarian Cancer. Clin Cancer Res. 2015.
21. Kalluri R, Zeisberg M. Fibroblasts in cancer. Nat Rev Cancer. 2006;6:392-401.
22. Mouw JK, Ou G, Weaver VM. Extracellular matrix assembly: a multiscale deconstruction. Nat Rev Mol Cell Biol. 2014;15:771-85.
23. Yeung TL, Leung CS, Wong KK, Samimi G, Thompson MS, Liu J, et al. TGF-beta modulates ovarian cancer invasion by upregulating CAF-derived versican in the tumor microenvironment. Cancer Res. 2013;73:5016-28.
24. Iwano M, Plieth D, Danoff TM, Xue C, Okada H, Neilson EG. Evidence that fibroblasts derive from epithelium during tissue fibrosis. J Clin Invest. 2002;110:341-50.
25. Petersen OW, Nielsen HL, Gudjonsson T, Villadsen R, Rank F, Niebuhr E, et al. Epithelial to mesenchymal transition in human breast cancer can provide a nonmalignant stroma. Am J Pathol. 2003;162:391-402.
26. Isella C, Terrasi A, Bellomo SE, Petti C, Galatola G, Muratore A, et al. Stromal contribution to the colorectal cancer transcriptome. Nat Genet. 2015;47:312-9.
27. Calon A, Lonardo E, Berenguer-Llergo A, Espinet E, Hernando-Momblona X, Iglesias M, et al. Stromal gene expression defines poor-prognosis subtypes in colorectal cancer. Nat Genet. 2015;47:320-9.
28. Schauer IG, Sood AK, Mok S, Liu J. Cancer-associated fibroblasts and their putative role in potentiating the initiation and development of epithelial ovarian cancer. Neoplasia. 2011;13:393-405.
29. Saad AF, Hu W, Sood AK. Microenvironment and pathogenesis of epithelial ovarian cancer. Horm Cancer. 2010;1:277-90.
30. Farmer P, Bonnefoi H, Anderle P, Cameron D, Wirapati P, Becette V, et al. A stroma-related gene signature predicts resistance to neoadjuvant chemotherapy in breast cancer. Nat Med. 2009;15:68-74.
31. Wynn TA, Ramalingam TR. Mechanisms of fibrosis: therapeutic translation for fibrotic disease. Nat Med. 2012;18:1028-40.

- **4) Other Achievements**

We identified ADAM metallopeptidase domain 12 (ADAM12) as one of the genes associated with poor survival in HGSOC (Table 1). ADAM12 is a promising biomarker because of its low expression in normal tissues and high expression in a variety of human cancers. Moreover, a serum-based ADAM12 ELISA kit is commercially available, providing an opportunity to test the effectiveness of predicting survival based on preoperative serum levels of ADAM12. The results of testing ADAM12 as a biomarker in ovarian cancer are shown in the attached manuscript (Cheon et al., Carcinogenesis, 2015, in press) and are briefly described below.

We showed that high protein levels of ADAM12 in banked preoperative sera were associated with shorter progression-free and overall survival. Tumor levels of ADAM12 mRNA were also associated with shorter progression-free and overall survival as well as with lymphatic and vascular invasion and residual tumor volume following cytoreductive surgery. The majority of genes co-expressed with ADAM12 in HGSOC were TGFβ signaling targets that function in collagen remodeling and cell-matrix adhesion. In tumor sections, the ADAM12 protein and mRNA were expressed in epithelial cancer cells and surrounding stromal cells. *In vitro* data showed that ADAM12 mRNA levels can be increased by TGFβ signaling and direct contact between epithelial and stromal cells.

High tumor levels of ADAM12 mRNA were characteristic of the mesenchymal/desmoplastic molecular subtype of HGSOC, which is known to have the poorest prognosis. Thus, ADAM12 may be a useful serum biomarker of aggressive ovarian cancer for which standard treatment is ineffective.

- **What opportunities for training and professional development has the project provided?**

Nothing to Report.

- **How were the results disseminated to communities of interest?**

Nothing to Report.

- **What do you plan to do during the next reporting period to accomplish the goals?**

Over the next year, we will validate the computationally-derived gene signatures by generating Nanostring data from formalin-fixed paraffin-embedded patient samples. Using statistical and molecular methods, we will correlate the data with overall survival, progression-free survival, residual disease status and other outcomes that could be used to improve the clinical management of ovarian cancer patients. Finally, we will develop a preliminary quantitative assay for use in the clinical setting.

4. **IMPACT:**

- **What was the impact on the development of the principal discipline(s) of the project?**

Nothing to Report.

- **What was the impact on other disciplines?**

Nothing to Report.

- **What was the impact on technology transfer?**

Nothing to Report.

- **What was the impact on society beyond science and technology?**

Nothing to Report.

5. **CHANGES/PROBLEMS:**

- **Changes in approach and reasons for change**

Nothing to Report.

- **Actual or anticipated problems or delays and actions or plans to resolve them**

We have experienced some delays in the molecular analysis of tumor samples because of our postdoctoral fellow's departure and the requisite training of new staff members. Prior to the postdoctoral fellow's departure in March 2015, she trained one postdoctoral fellow and one research assistant in the Orsulic laboratory to enable continuity of the project until a new postdoctoral fellow joined the laboratory in May 2015. The new postdoctoral fellow is currently being trained to assume the tasks on the project.

Changes that had a significant impact on expenditures

Nothing to Report.

- **Significant changes in use or care of human subjects, vertebrate animals, biohazards, and/or select agents**

Nothing to Report.

6. **PRODUCTS:**

- **Journal publications.**

Cheon DJ, Li AJ, Beach JA, Walts AE, Tran H, Lester J, Karlan BY, Orsulic S. ADAM12 is a prognostic factor associated with an aggressive molecular subtype of high grade serous ovarian carcinoma. Carcinogenesis 2015, in press; acknowledgement of federal support (yes).

- **Inventions, patent applications, and/or licenses**

Research from this project was added as "in-part" additional data to the following patent:
Orsulic S, Liu Z, Karlan BY, Cui X, Tighiouart M, Cheon D-J. Molecular Signatures of Ovarian Cancer, 14/690,291; filed April 17, 2015

7. **PARTICIPANTS & OTHER COLLABORATING ORGANIZATIONS**

- **What individuals have worked on the project?**

The following individuals have contributed at least one person month on the project:

Name:	Sandra Orsulic
Project Role:	PI
Nearest person month worked:	1.2
Contribution to Project:	Dr. Orsulic oversaw statistical analyses of the gene signatures, analyzed and interpreted the data, wrote and published one manuscript, and prepared another one for publication.

Name:	Dong Joo Cheon
Project Role:	Postdoctoral fellow
Nearest person month worked:	3
Contribution to Project:	Dr. Cheon organized retrieval of pathology samples, isolated RNA and prepared cDNA from samples, optimized qPCR, and assisted in the writing of the published manuscript.

- **Has there been a change in the active other support of the PD/PI(s) or senior/key personnel since the last reporting period?**

One postdoctoral fellow accepted an independent faculty position at another institution and has been replaced by a new postdoctoral fellow.

- **What other organizations were involved as partners?**

Nothing to Report.

8. **SPECIAL REPORTING REQUIREMENTS**

N/A

9. **APPENDICES:**

Journal article in press: Cheon et al., Carcinogenesis, 2015

OXFORD

Carcinogenesis, 2015, 1–9

doi:10.1093/carcin/bgv059
Original Manuscript

ORIGINAL MANUSCRIPT

ADAM12 is a prognostic factor associated with an aggressive molecular subtype of high-grade serous ovarian carcinoma

Dong-Joo Cheon[1], Andrew J.Li[1,2], Jessica A.Beach[1,3], Ann E.Walts[4], Hang Tran[1], Jenny Lester[1], Beth Y.Karlan[1,2] and Sandra Orsulic[1,2,*]

[1]Women's Cancer Program, Samuel Oschin Comprehensive Cancer Institute, Cedars-Sinai Medical Center, Los Angeles, CA 90048, USA, [2]Department of Obstetrics and Gynecology, David Geffen School of Medicine, University of California at Los Angeles, Los Angeles, CA 90095, USA and [3]Gradute Program in Biomedical Science and Translational Medicine and [4]Department of Pathology and Laboratory Medicine, Cedars-Sinai Medical Center, Los Angeles, CA 90048, USA

*To whom correspondence should be addressed. Tel: 310-423-9546; Fax: 310-423-9537;Email: Sandra.Orsulic@cshs.org

Abstract

ADAM metallopeptidase domain 12 (ADAM12) is a promising biomarker because of its low expression in normal tissues and high expression in a variety of human cancers. However, ADAM12 levels in ovarian cancer have not been well characterized. We previously identified *ADAM12* as one of the signature genes associated with poor survival in high-grade serous ovarian carcinoma (HGSOC). Here, we sought to determine if high levels of the ADAM12 protein and/or messenger RNA (mRNA) are associated with clinical variables in HGSOC. We show that high protein levels of ADAM12 in banked preoperative sera are associated with shorter progression-free and overall survival. Tumor levels of ADAM12 mRNA were also associated with shorter progression-free and overall survival as well as with lymphatic and vascular invasion, and residual tumor volume following cytoreductive surgery. The majority of genes co-expressed with ADAM12 in HGSOC were transforming growth factor (TGF)β signaling targets that function in collagen remodeling and cell–matrix adhesion. In tumor sections, the ADAM12 protein and mRNA were expressed in epithelial cancer cells and surrounding stromal cells. *In vitro* data showed that ADAM12 mRNA levels can be increased by TGFβ signaling and direct contact between epithelial and stromal cells. High tumor levels of ADAM12 mRNA were characteristic of the mesenchymal/desmoplastic molecular subtype of HGSOC, which is known to have the poorest prognosis. Thus, ADAM12 may be a useful biomarker of aggressive ovarian cancer for which standard treatment is not effective.

Introduction

ADAM metallopeptidase domain 12 (*ADAM12*) encodes a member of the ADAM (a disintegrin and metalloprotease) protein family. In humans, two isoforms of ADAM12 (also known as meltrin-α) exist as a result of alternative messenger RNA (mRNA) splicing: a long transmembrane form (ADAM12-L) and a truncated secreted form lacking the transmembrane and cytoplasmic domains (ADAM12-S). Both ADAM12-L and ADAM12-S are proteolytically processed, and the mature forms translocate to the plasma membrane and extracellular space, respectively (1), to assume their proteolytic function (2–5).

Multiple studies have demonstrated that increased levels of ADAM12 correlate with tumor progression but it is unknown if ADAM12 is an actual perpetrator in tumor progression. In mouse models of breast and prostate cancers, tumor growth and metastasis were diminished in ADAM12$^{-/-}$ mice in comparison with wild-type littermates, indicating that ADAM12 may be required for tumor progression (6,7). Overexpression studies also support the role of ADAM12 in tumor progression and provide mechanistic insight into the relevance of its adhesion and proteolytic functions (8–12).

Received: February 5, 2015; **Revised:** April 9, 2015; **Accepted:** April 26, 2015

Abbreviations

ADAM12	ADAM metallopeptidase domain 12
ELISA	enzyme-linked immunosorbent assay
HGSOC	high-grade serous ovarian carcinoma
mRNA	messenger RNA
TGF	transforming growth factor

ADAM12 has attracted attention as a biomarker because of its restricted expression in normal tissues and considerable activation in various disease processes. Aside from high expression in the human placenta and transient expression during embryonic morphogenesis of muscle and bone (5), postnatal ADAM12 expression in healthy and non-injured organs is low. However, levels of ADAM12 are elevated in diseases accompanied by fibrosis (13). Further, increased levels of ADAM12 have been reported in human cancers including cancers of the breast (6,14–16), liver (17–22), head and neck (11,23,24), stomach (25), bladder (26), prostate (7), lung (27), brain (28) and bone (29).

ADAM12 has not been examined as a potential biomarker in ovarian cancer. However, ADAM12 was identified in an unbiased screen as one of the transmembrane proteins expressed in ovarian tumor vasculature but not the vasculature of normal ovaries (30). In the same study, it was noted that expression of ADAM12 was highly variable among ovarian cancers, with high expression in some samples and minimal expression in others, suggesting that ADAM12 might serve as a biomarker in ovarian cancer (30). We previously identified gene signatures associated with poor survival in high-grade serous ovarian carcinoma (HGSOC) (31,32). Since *ADAM12* was among the signature genes, we hypothesize that high levels of ADAM12 are associated with adverse outcome in HGSOC.

Methods

Patient samples

Studies involving human specimens were approved by the Cedars-Sinai Medical Center Institutional Review Board. All patients signed an institutional review board-approved consent for biobanking, clinical data extraction and molecular analysis. Banked frozen preoperative sera were obtained from the Women's Cancer Program Bioepository and prepared for analysis as described in our previous publications (33,34). All patients in this study had advanced stage (FIGO III or IV), high-grade (2 or 3) serous ovarian carcinoma. Patients with other malignancies, borderline ovarian tumors and ovarian tumors of non-epithelial histology were excluded. All patients underwent initial surgical exploration with the intent of optimal cytoreduction (defined as residual disease <1 cm) and were treated with at least six cycles of platinum-based chemotherapy. Patients who received intraperitoneal chemotherapy or underwent neoadjuvant chemotherapy were excluded. Immunohistochemical staining and *in situ* hybridization were performed on formalin-fixed, paraffin-embedded tumors surgically removed from patients and obtained from the Pathology Department archives.

Enzyme-linked immunosorbent assay

A solid-phase enzyme-linked immunosorbent assay (ELISA) was performed using the Quantikine human ADAM12 ELISA kit (R&D Systems) following the manufacturer's instructions. Briefly, 100 µl of Assay Diluent was added to each well of the 96-well plate precoated with a monoclonal antibody specific for human ADAM12. Fifty microliters of ADAM12 standard (0–100 ng/ml) or patient sera were added to each well and incubated for 2 h at room temperature on a horizontal orbital microplate shaker (500 r.p.m.). The liquids were carefully discarded and the wells were washed four times with 400 µl of the Wash Buffer. Two hundred microliters of ADAM12 Conjugate, an enzyme-linked monoclonal antibody specific for human ADAM12, was added to each well and incubated for 2 h at room temperature on the shaker. After washing four times with the Wash Buffer, 200 µl of Substrate Solution was added to each well and incubated for 30 min at room temperature. The color development was stopped by adding 50 µl of Stop Solution to each well and the optical density at 450 nm was measured by a microplate reader. ADAM12 concentration (ng/ml) in patient sera was calculated by a formula obtained from the ADAM12 standard curve.

Immunohistochemical staining and *in situ* hybridization

Immunohistochemical detection of ADAM12 was performed using the Vectastatin Elite ABC kit with rabbit immunoglobulin G (Vector Laboratories) following the manufacturer's instructions. Formalin-fixed, paraffin-embedded tissue sections were deparaffinized and rehydrated in a series of xylene and diluted alcohol. Antigen retrieval was performed by boiling the slides in the Antigen Unmasking Solution (Vector Laboratories). Endogenous peroxidase was inactivated by a 30 min incubation in 0.3% H_2O_2 solution in methanol. After blocking with goat serum, a polyclonal ADAM12 Prestige Antibody (Sigma–Aldrich) was incubated at 1:150 dilution for 30 min at room temperature. Slides were washed and incubated with the biotinylated rabbit immunoglobulin G for 30 min at room temperature. After washing, the slides were incubated with the ABC reagent for 30 min at room temperature, then incubated in the ImmPACT DAB (Vector Laboratories) for 8 min, counterstained with Harris hematoxylin (Sigma–Aldrich), dehydrated and mounted with Permount (Fisher Scientific).

ADAM12 *in situ* hybridization was performed using RNAscope 2.0 FFPE Assay (Advanced Cell Diagnostics) as described in Cheon *et al.* (31). Slides were examined using the Olympus BX43 upright microscope (Olympus).

Cell culture

The OVCAR3 ovarian cancer cell line was obtained from Dennis Slamon (University of California, Los Angeles). All other ovarian cancer cell lines were purchased from the American Type Culture Collection (Manassas, VA). Cell line authenticity was confirmed by Laragen using the short tandem repeat method. The TRS3 normal ovarian stroma cell line was generated as described previously (31). The ovarian cancer cells and TRS3 cells were cultured in Dulbecco's modified Eagle's medium (Corning) and a 1:1 mixture of MCDB 105 (Sigma) and 199 (Gibco) media, respectively, supplemented with 10% fetal bovine serum and 1% penicillin–streptomycin. Ovarian cancer cells were cocultured for 48 h with TRS3 cells using Millicell 6-well inserts with 0.4 µm PET membrane (Merck Millipore). Alternatively, green fluorescent protein (GFP)-labeled ovarian cancer cells were cultured on a monolayer of TRS3 cells for 48 h and GFP+ cells were sorted using the BD FACSAria™ III cell sorter (BD Biosciences) by the Cedars-Sinai Medical Center flow cytometry core staff. For transforming growth factor (TGF)β1 treatment, 10^5 cells were plated in six-well plates, serum-starved overnight, then incubated with 10 ng/ml TGFβ1 (Sigma) for 48 h before harvesting.

RNA isolation and quantitative real-time PCR analysis

Total RNA was extracted using the RNeasy mini kit (Qiagen) and was reverse-transcribed to complementary DNA using the QuantiTect Reverse Transcription Kit (Qiagen). A total of 50 ng of complementary DNA was mixed with primers and iQ SYBR Green Supermix (Bio-Rad) in a 96-well plate format. For primers, the RT^2 qPCR Primer Assay for Human ADAM12 (Qiagen; PPH07647A) and the ribosomal protein L32 (internal control) (Forward: 5′-ACAAAGCACATGCTGCCCAGTG-3′; Reverse: 5′-TTCCACGATGGCTTTGCGGTTC-3′) were used. The quantitative reverse transcription–PCR reaction was performed using a CFX96 thermo cycler (Bio-Rad) and the data were analyzed by the $2^{-\Delta CT}$ method. Samples were in triplicate and the experiment was repeated twice.

Statistical methods

Abstracted data from medical charts included age, stage, grade, status of cytoreductive surgery and time to recurrence and death. For statistical considerations, we defined an elevated ADAM12 level as >1.0 ng/ml. Differences in clinical and histopathologic factors between patients with high and low serum ADAM12 were examined with chi-square and Fisher's exact test. The Cox regression analysis was performed to assess the significance of potential prognostic factors. Patient survival was analyzed

with Kaplan–Meier curves. A *P* value of <0.05 was considered statistically significant.

Analyses of public databases

R2 (http://hgserver1.amc.nl/) was used to statistically analyze and graph data from public microarray data sets. The Kaplan–Meier online plotter tool (http://kmplot.com/analysis/) was used to generate survival curves by combining ADAM12 mRNA data from serous ovarian cancer patients from 13 public ovarian cancer data sets (Supplementary Table I is available at *Carcinogenesis* Online). cBioPortal (http://www.cbioportal.org/) was used to identify ADAM12-correlated transcripts in the ovarian cancer TCGA data set. DAVID (http://david.abcc.ncifcrf.gov/) and Ingenuity Pathway Analysis were used for functional annotation of the transcripts and identification of upstream regulators, respectively.

Results

High serum protein levels of ADAM12 are associated with poor survival in patients with HGSOC

Eighty-four patients with HGSOC met the criteria for inclusion in the study. All patients underwent initial surgical cytoreduction followed by adjuvant chemotherapy. The majority of patients had grade 3, stage III disease and were optimally resected (residual disease <1 cm). ADAM12 levels in banked preoperative sera were determined by ELISA. The protein levels ranged from 0 to 5.76 ng/ml with an average of 1.06 ng/ml and a median of 0.83 ng/ml. We arbitrarily selected 1 ng/ml as a cutoff to divide the 84 patients into two groups: 48 patients with low (<1 ng/ml; range 0.00–0.98 ng/ml) and 36 patients with high (>1 ng/ml; range 1.03–5.76 ng/ml) levels of ADAM12. The distribution of cohort characteristics between patients with low and high levels of ADAM12 are shown in Supplementary Table II is available at *Carcinogenesis* Online.

In order to determine if serum ADAM12 levels correlate with clinical outcome, we used Kaplan–Meier analyses for both time to first recurrence and time to death. Women with low serum ADAM12 levels had a longer median progression-free survival than those with high ADAM12 levels (21 months versus 14 months, *P* = 0.037) (Figure 1A). Similarly, women with low ADAM12 levels had a longer median overall disease-specific survival than those with high ADAM12 levels (57 months versus 45 months, *P* = 0.033) (Figure 1A). The significance of ADAM12 as

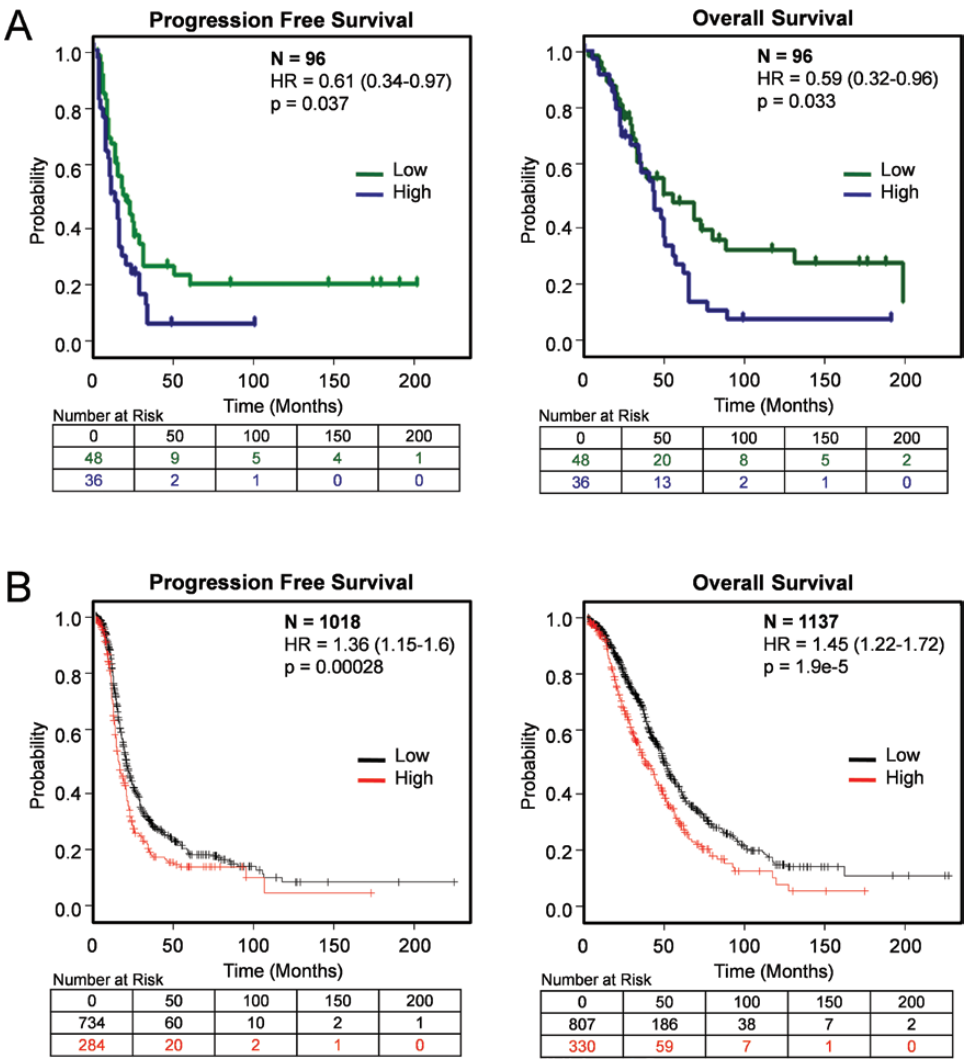

Figure 1. Kaplan–Meier survival curves in serous ovarian carcinoma patients with low and high levels of ADAM12. (**A**) Survival curves in HGSOC patients with low (<1 ng/ml) and high (>1 ng/ml) preoperative serum levels of ADAM12. (**B**) Survival curves in serous ovarian cancer patients with low and high expression levels of ADAM12 mRNA (202952_s_at) from 13 combined public ovarian cancer data sets in the Kaplan–Meier plotter database.

an independent prognostic factor was evaluated by Cox regression analysis. ADAM12 levels retained statistical significance ($P = 0.02$, risk ratio 1.36, confidence intervals 1.06–1.75) after controlling for age, stage (III or IV), grade (2 or 3) and cytoreduction status (optimal or suboptimal) (Supplementary Table III is available at *Carcinogenesis* Online).

ADAM12 mRNA levels are associated with poor patient survival, increased tumor invasion and decreased success in surgical cytoreduction

The existence of multiple expression profile data sets for ovarian cancer facilitated the correlative analysis of ADAM12 mRNA levels with clinical parameters in a large number of patients. High levels of ADAM12 mRNA were associated with poor progression-free and overall survival in a cohort of serous ovarian cancer patients that integrated data from 13 different data sets (Figure 1B). To determine whether levels of ADAM12 correlate with various clinical parameters, we used the ovarian cancer TCGA data set (35). ADAM12 mRNA levels correlated with lymphatic invasion, venous invasion and size of residual tumor after cytoreductive surgery (Figure 2), whereas there was no statistically significant correlation with tumor stage, tumor grade, patient age at diagnosis, performance status, race or ethnicity (data not shown).

ADAM12 mRNA levels are associated with the mesenchymal/desmoplastic molecular subtype of ovarian carcinoma

Since high serum and mRNA levels of ADAM12 were associated with worse clinical outcomes, we hypothesized that tumors in HGSOC patients with high levels of ADAM12 would exhibit aggressive biology, including increased invasion, suboptimal cytoreduction and poor survival. To determine if high levels of ADAM12 were associated with a specific molecular subtype of HGSOC, we used the ovarian cancer TCGA data set from 489 patients with HGSOC (35). Based on expression profiles, the

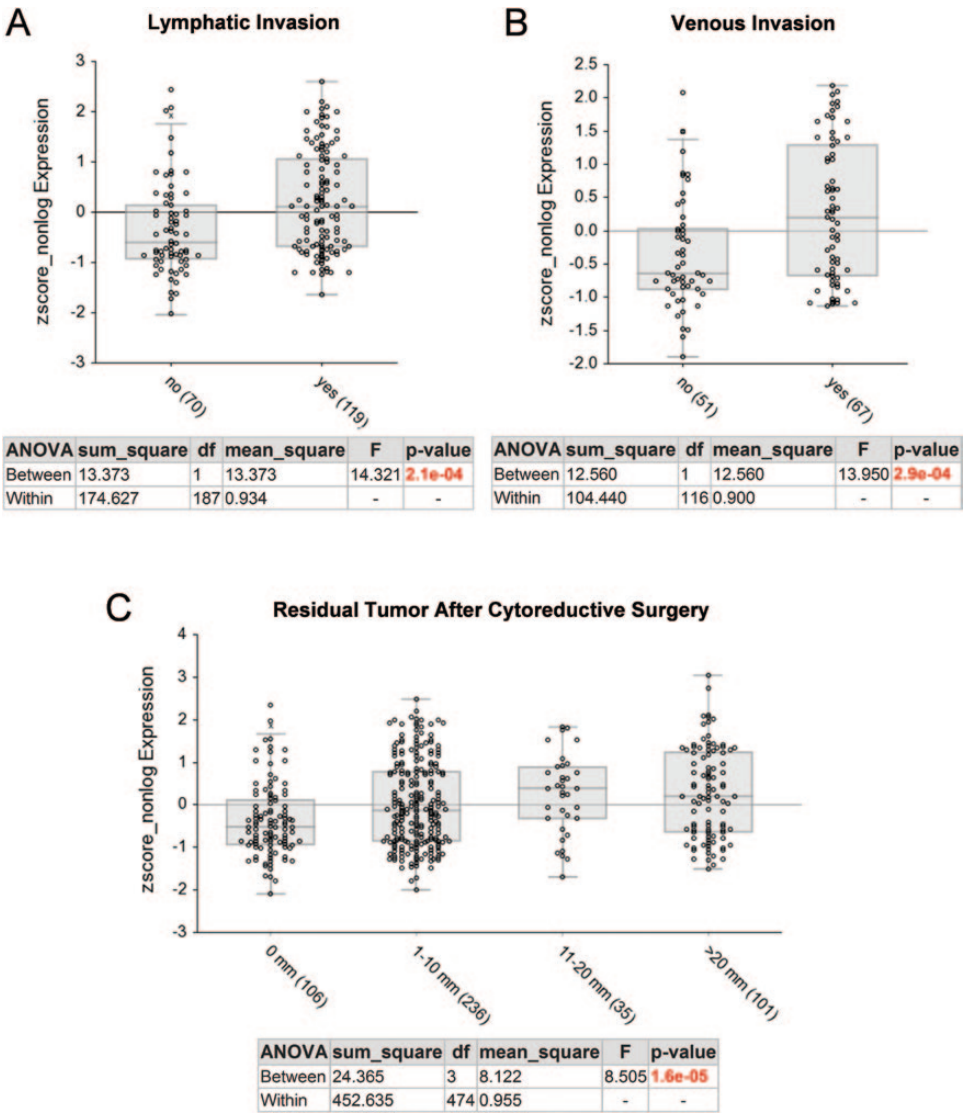

ANOVA	sum_square	df	mean_square	F	p-value
Between	13.373	1	13.373	14.321	2.1e-04
Within	174.627	187	0.934	-	-

ANOVA	sum_square	df	mean_square	F	p-value
Between	12.560	1	12.560	13.950	2.9e-04
Within	104.440	116	0.900	-	-

ANOVA	sum_square	df	mean_square	F	p-value
Between	24.365	3	8.122	8.505	1.6e-05
Within	452.635	474	0.955	-	-

Figure 2. Comparison of ADAM12 expression levels and clinicopathological parameters in the ovarian cancer TCGA data set. (**A**) Lymphatic invasion, (**B**) Venous invasion, (**C**) Residual tumor after cytoreductive surgery. The graphs and statistical data were generated using R2 Genomics Analysis and Visualization Platform. The *x*-axis shows individual groups where the number of patients in each group is indicated in parentheses. The *y*-axis represents a relative value of ADAM12 mRNA (202952_s_at) expression.

cancer samples in this data set have been clustered into four molecular subtypes: differentiated, immunoreactive, mesenchymal and proliferative (35). Strikingly, almost all tumors of the mesenchymal subtype had elevated levels of ADAM12 (Figure 3A). Similarly in the Tothill data set, 259 serous and endometrioid ovarian carcinomas have been clustered based on their expression profile into six distinct molecular subtypes (C1–C6) (36). The C1 subtype has been characterized by a reactive stroma gene expression signature and was shown to be enriched in tumors with extensive desmoplasia (36). Almost all tumors in the C1 subtype exhibited elevated levels of ADAM12 (Figure 3B).

ADAM12 is expressed in epithelial cancer cells and surrounding stromal cells and can be induced by epithelial–stromal interaction and TGFβ signaling

To better understand the biology of the tumors with high levels of ADAM12, we identified gene transcripts that most closely correlate with expression of ADAM12 in the ovarian cancer TCGA data set. The majority of the ADAM12-correlated genes were matricellular and extracellular matrix proteins, such as collagens and collagen-remodeling enzymes (Table 1), which we previously identified as part of a gene signature of poor survival in HGSOC (31). Gene Ontology analysis showed that ADAM12-correlated genes are primarily involved in collagen remodeling, tissue development and cell adhesion (Table 2).

To evaluate the cellular localization of ADAM12 in tumors, an ADAM12-specific polyclonal antibody and an ADAM12-specific probe were used to perform immunohistochemical staining and *in situ* hybridization on tumor sections from several of our patients with HGSOC. ADAM12 protein and mRNA were detected in tumor epithelial cells and adjacent stromal cells but not in distant (>1 mm) stromal cells (Figure 4A). To determine if ADAM12 expression is induced by an interaction between stromal and cancer cells, SV40 large T-antigen-transformed stromal cells from a normal ovary (TRS3) were cocultured with a panel of ovarian cancer cell lines (OVCAR3, OVCAR433, HEY and SKOV3). OVCAR3 and OVCAR433 cells have a cobblestone morphology characteristic of epithelial cells (Figure 4B) and have been classified as 'epithelial' and 'intermediate epithelial' cells, respectively, based on their expression of epithelial markers and low migratory and invasive potential (37). We have demonstrated in OVCAR3 cells that their migration and invasion can be augmented by coculture with stromal TRS3 cells (J.A.Beach *et al*. in preparation). In contrast, HEY and SKOV3 cells are more elongated and spindle-shaped (Figure 4B) and have been classified as 'intermediate mesenchymal' cells based on their expression of mesenchymal markers and high migratory and invasive potential (37). We observed that the epithelial OVCAR3 and OVCAR433 cell lines had low levels of ADAM12 mRNA that could be significantly induced by both direct and indirect coculture with TRS3 stromal cells (Figure 4C). Conversely, mesenchymal HEY and SKOV3 cell lines had high levels of ADAM12 mRNA that were similar to that of TRS3 stromal cells. Further, neither direct nor indirect coculture with TRS3 cells significantly altered ADAM12 mRNA levels in HEY and SKOV3 cells (Figure 4C). Ingenuity Pathway Analysis revealed that many of the ADAM12-correlated genes in Table 1 are expressed in tumor stroma and are downstream targets of TGFβ (data not shown), indicating that ADAM12 may be regulated by TGFβ signaling. Consistent with this idea, ADAM12 levels in TRS3 cells increased ~10-fold in the presence of recombinant TGFβ1 and were further increased by direct coculture with OVCAR3 cells (Figure 4D).

Discussion

Several cancer studies have demonstrated the potential utility of ADAM12 as a diagnostic and prognostic marker. For example,

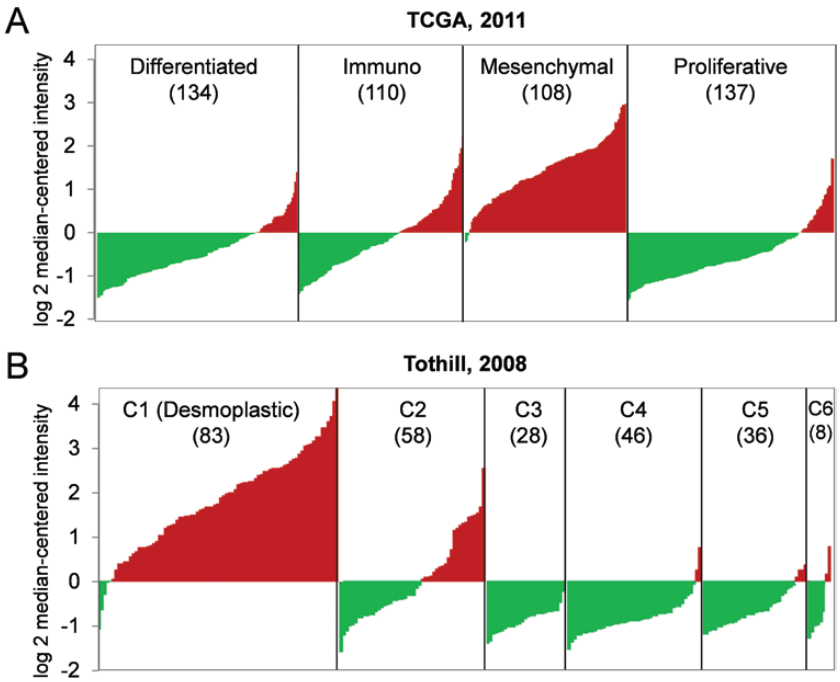

Figure 3. Association of high expression levels of ADAM12 with a specific molecular subtype of ovarian carcinoma. A diagram of ADAM12 mRNA distribution in (**A**) 489 serous ovarian carcinomas in the ovarian cancer TCGA data set grouped into four distinct molecular subtypes and (**B**) 259 ovarian serous and endometrioid carcinomas in the Tothill data set grouped into six distinct molecular subtypes. The *x*-axis shows individual tumors that are merged into a continuous plot (the number of tumor samples in each subtype is indicated in parentheses). The *y*-axis represents a relative value of mRNA expression. Red indicates positive values, green indicates negative values.

western blot analysis showed elevated levels of ADAM12 in urine from patients with breast cancer compared with healthy control subjects (38). In addition to detecting the presence of breast cancer, the urine levels of the ADAM12 protein also correlated with tumor stage and progressively increased from patients with *in situ* carcinoma to locally invasive cancer to metastatic disease (38). Similarly, urine protein levels of ADAM12 were significantly increased in patients with bladder cancer compared with healthy controls (26). In the breast cancer study and bladder cancer study, the levels of ADAM12 mRNA and protein increased as a function of cancer stage, with the highest levels found in the largest invasive tumors (26). In the small number of bladder cancer patients studied, urine protein levels of ADAM12 decreased following tumor resection and increased again upon tumor recurrence, providing further support for the diagnostic utility of ADAM12 (26).

Table 1. Genes co-expressed with ADAM12 in the ovarian cancer TCGA data set.

Correlated gene	Pearson's correlation	Spearman's correlation
COL5A2	0.89	0.78
COL3A1	0.88	0.9
POSTN	0.88	0.85
COL5A1	0.87	0.84
ADAMTS12	0.87	0.84
THBS2	0.87	0.8
COL1A1	0.85	0.86
SPARC	0.84	0.85
VCAN	0.84	0.8
COL11A1	0.84	0.77
FAP	0.83	0.85
MMP2	0.83	0.85
LUM	0.83	0.79
ADAMTS2	0.83	0.78
CRISPLD2	0.83	0.71
FN1	0.83	0.7
INHBA	0.83	0.58
OLFML2B	0.82	0.81
COL6A3	0.82	0.78
ECM1	0.82	0.78
SNAI2	0.82	0.71
KCNE4	0.82	0.7
MMP11	0.82	0.68
COL5A3	0.82	0.67
ALPK2	0.81	0.74
PRRX1	0.81	0.35
COL1A2	0.8	0.87
LOX	0.79	0.78
CHSY3	0.79	0.77
LRRC15	0.79	0.74

Agilent microarray, 489 ovarian cancer samples.

In the current study, we identified significant differences in progression-free and overall survival between women with high and low serum ADAM12 levels in a cohort of patients with stage III/IV HGSOC. Multivariable analyses identified serum ADAM12 as an independent prognostic factor for survival. The presence of lymphovascular invasion is an important predictor of poor survival in ovarian cancer (39). We showed that ADAM12 mRNA levels correlate with lymphatic and vascular invasion in the ovarian cancer TCGA data set, supporting the hypothesis that tumors with high levels of ADAM12 are biologically aggressive. Another important predictor of survival is the extent of residual disease after primary cytoreductive surgery (40). We showed that tumor ADAM12 mRNA levels correlate with the extent of residual disease in the ovarian cancer TCGA data set, suggesting that ADAM12 may be a biomarker of unresectable ovarian cancer. However, such a biomarker would be useful only if it can stratify patients preoperatively. In cases where the extent of ovarian cancer precludes optimal resection, efforts are made to reduce tumor burden with neoadjuvant chemotherapy prior to interval cytoreductive surgery (41). Currently, there is no clinical biomarker that can be applied preoperatively to predict when optimal or suboptimal cytoreduction can be surgically accomplished. Since the majority of patients in our cohort were optimally cytoreduced, we were unable to assess the ability of preoperative serum levels of ADAM12 to predict suboptimal cytoreduction. Considering the correlation of tumor ADAM12 mRNA with residual tumor volume and the correlation of preoperative serum ADAM12 protein with poor survival, a study that directly correlates serum ADAM12 with residual disease is warranted. An effective serum biomarker of suboptimal cytoreduction would impact the management of ovarian cancer patients as they could be spared a suboptimal surgical procedure and directly triaged to neoadjuvant chemotherapy (41).

Outcome predictors based on a molecular subtype rather than surgical staging have been successfully applied in breast cancer where gene signatures are used to predict metastasis and recurrence and to identify patients who are more likely to respond to a specific therapy. In breast cancer, it has been shown that ADAM12 is predominantly upregulated in claudin-low

Table 2. Functional annotation of genes co-expressed with ADAM12 in the ovarian cancer TCGA data set

GO term	Count	%	*P* value	Genes
GO:0030199~collagen fibril organization	7	23.3333	1.25E-11	LUM, COL3A1, COL1A1, COL5A3, COL5A2, COL11A1, COL5A1
GO:0001501~skeletal system development	11	36.6667	1.76E-10	INHBA, CTSK, FBN1, COL3A1, PRRX1, POSTN, SPARC, COL1A1, COL5A2, COL11A1, MMP2
GO:0032963~collagen metabolic process	5	16.6667	2.13E-07	COL3A1, COL1A1, MMP2, COL5A1, MMP11
GO:0043588~skin development	5	16.6667	2.46E-07	COL3A1, COL1A1, COL5A3, COL5A2, COL5A1
GO:0007155~cell adhesion	10	33.3333	3.56E-06	COL6A3, COL3A1, ITGA11, VCAN, POSTN, COL5A3, THBS2, COL11A1, COL5A1, FN1
GO:0007160~cell–matrix adhesion	4	13.3333	6.41E-04	COL3A1, ITGA11, COL5A3, FN1

GO, Gene Ontology.

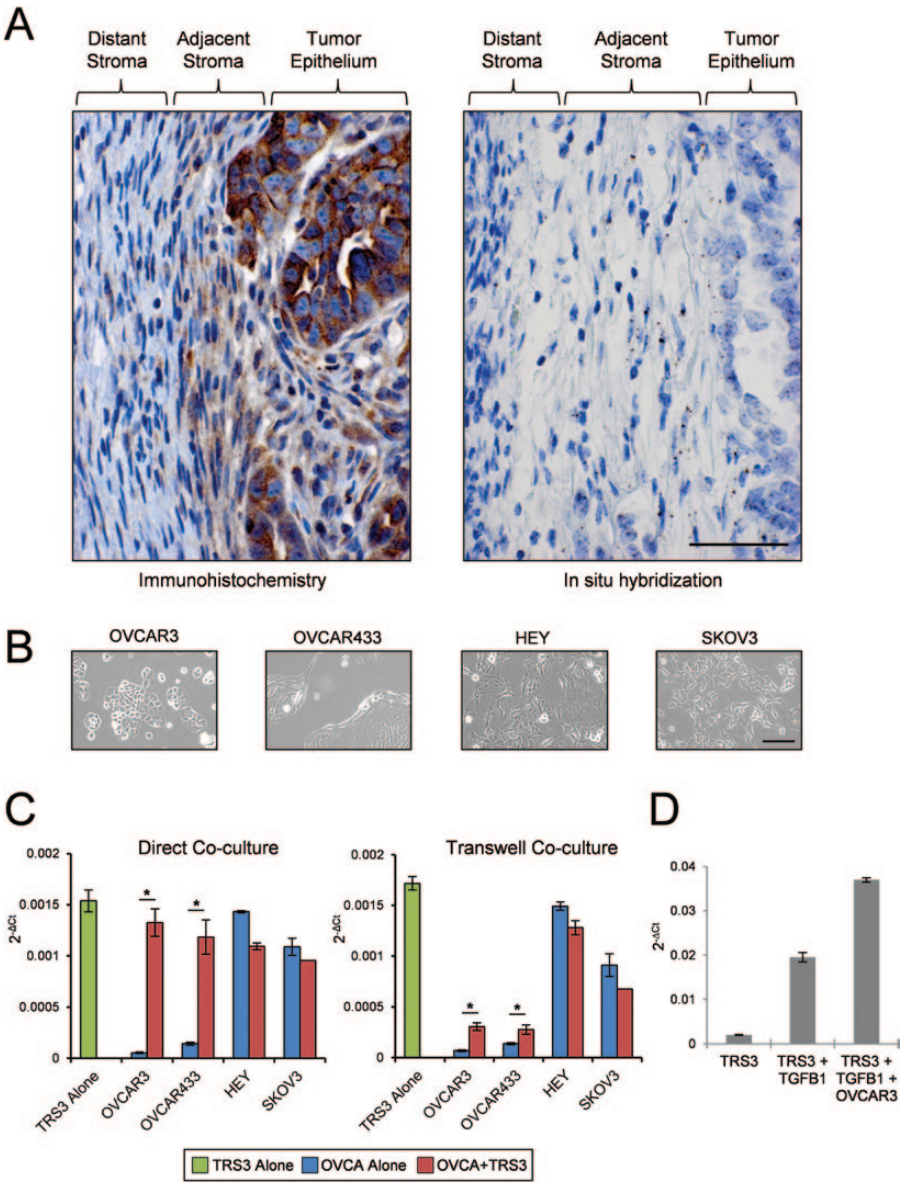

Fig. 4. ADAM12 expression in epithelial and stromal cells in patient tumors and different culture conditions. (**A**) Representative localization of ADAM12 protein (immunohistochemistry; brown staining) and mRNA (*in situ* hybridization; brown dots) in ovarian tumor sections from HGSOC patients. Size bar for both photographs = 50 μm. (**B**) Bright field microscopy depicting cell morphology of ovarian cancer (OVCA) cell lines. Size bar = 100 μm. (**C**) Quantitative real-time PCR of ADAM12 mRNA levels in the TRS3 ovarian stromal cell line and various OVCA cell lines alone or in coculture. TRS3 cells and GFP-labeled OVCA cells were cocultured in direct contact or indirectly via transwell inserts for 48 h. (**D**) Quantitative real-time PCR of ADAM12 mRNA in the TRS3 cells alone or in coculture with OVCAR3 epithelial cells in the presence or absence of 10 ng/ml of recombinant TGFβ1. Data are normalized to ribosomal protein L32 and represent the mean ± SEM. *$P < 0.05$.

tumors, an aggressive subtype that exhibits molecular signatures of breast tumor-initiating cells and cells undergoing epithelial to mesenchymal transition (18,19,42). In the ovarian cancer TCGA data set (35) and the Tothill data set (36), we observed that high levels of ADAM12 were associated with the mesenchymal and the C1/desmoplastic subtype, respectively. Notably, these subtypes have been associated with the poorest survival when compared with other molecular subtypes in each data set (36,43,44). A common characteristic of both the mesenchymal and C1/desmoplastic molecular subtypes is extensive desmoplasia. Consistent with this phenotype, the genes co-expressed with ADAM12 in HGSOC are known to be involved in collagen remodeling, tissue organization and cell adhesion. The mechanisms by which desmoplasia contributes to poor survival is still unclear. Possible mechanisms include the presence of a nurturing environment for cancer stem cells, formation of linear collagen tracks for efficient cancer cell migration and invasion and increased interstitial pressure that thwarts drug delivery (45). For effective and durable remission, desmoplastic tumors may require different treatment approaches that target both cancer and stromal cells. Thus, in addition to serving as a predictor of poor prognosis, ADAM12 may be a biomarker for an aggressive molecular subtype of ovarian cancer that requires aggressive treatment with current cytotoxic therapy and/or experimental therapies that target stromal cells.

An important aspect of understanding the biomarker potential of ADAM12 in malignancy involves identification of the cells that produce and secrete ADAM12. In a variety of cell culture

systems, ADAM12 expression both regulates, and can be induced by, TGFβ signaling (17,46,47). The source of ADAM12 expression within tumor tissue has been debated. Strong expression has been reported in malignant epithelial cells, stromal cells or both depending upon the cancer type and/or animal model studied (6,7,13,14,16,17,28,48,49). In a mouse model of prostate cancer where expression of SV40 large T-antigen is regulated by the prostate-specific probasin promoter, *in situ* hybridization demonstrated expression of ADAM12 in a subpopulation of stromal cells adjacent to prostate tumor glands (7). The ADAM12-positive stromal cells were morphologically different from adjacent spindle-shaped fibroblasts and were positive for both α-SMA and SV40 large T-antigen, indicating that they had undergone an epithelial to mesenchymal transition (7). Given the role of ADAM12 in myoblast fusion (2) and in the formation of trophoblast syncytia (50), stromal cells in the prostate that express both markers could have arisen by cell fusion. In ovarian cancer, we detected the ADAM12 mRNA and protein in tumor epithelial cells and adjacent stromal cells. In human tumor sections, it is impossible to track cells to determine if the ADAM12-positive stromal cells were derived from epithelial cells via epithelial to mesenchymal transition or cell fusion. Our *in vitro* coculture data support the hypothesis that ADAM12 mRNA is induced in both cell types upon direct contact. If this hypothesis is validated in other systems that effectively mimic the microenvironment in cancer, increased ADAM12 levels could be a useful readout for active epithelial-stromal signaling in cancer.

Supplementary material

Supplementary Tables I–III can be found at http://carcin.oxfordjournals.org/

Funding

The Office of the Assistant Secretary of Defense for Health Affairs through the Ovarian Cancer Research Program (Award No. W81XWH-14-1-0107 to S.O.); the American Cancer Society (RSG-10-252-01-TBG to S.O., SIOP-06-258-01-COUN to B.Y.K.); the Ovarian Cancer Research Fund Ann Schreiber Mentored Investigator Award administered by the University of California Office of the President's Tobacco-Related Disease Research Program to D.-J.C. Opinions, interpretations, conclusions and recommendations are those of the author and are not necessarily endorsed by the Department of Defense.

Acknowledgements

We thank S.Swartwood and the Cedars-Sinai Medical Center Biobank and Translational Research Core for *in situ* hybridization studies and K.Daniels for assistance in the preparation of the manuscript.
Conflict of interest statement: None declared.

References

1. Cao, Y. et al. (2002) Intracellular processing of metalloprotease disintegrin ADAM12. J. Biol. Chem., 277, 26403–26411.
2. Yagami-Hiromasa, T. et al. (1995) A metalloprotease-disintegrin participating in myoblast fusion. Nature, 377, 652–656.
3. Gilpin, B.J. et al. (1998) A novel, secreted form of human ADAM 12 (meltrin alpha) provokes myogenesis *in vivo*. J. Biol. Chem., 273, 157–166.
4. Hougaard, S. et al. (2000) Trafficking of human ADAM 12-L: retention in the trans-Golgi network. Biochem. Biophys. Res. Commun., 275, 261–267.
5. Kurisaki, T. et al. (1998) Spatially- and temporally-restricted expression of meltrin alpha (ADAM12) and beta (ADAM19) in mouse embryo. Mech. Dev., 73, 211–215.
6. Fröhlich, C. et al. (2011) ADAM12 produced by tumor cells rather than stromal cells accelerates breast tumor progression. Mol. Cancer Res., 9, 1449–1461.
7. Peduto, L. et al. (2006) ADAM12 is highly expressed in carcinoma-associated stroma and is required for mouse prostate tumor progression. Oncogene, 25, 5462–5466.
8. Díaz, B. et al. (2013) Notch increases the shedding of HB-EGF by ADAM12 to potentiate invadopodia formation in hypoxia. J. Cell Biol., 201, 279–292.
9. Albrechtsen, R. et al. (2011) Extracellular engagement of ADAM12 induces clusters of invadopodia with localized ectodomain shedding activity. Exp. Cell Res., 317, 195–209.
10. Roy, R. et al. (2011) Potential of fluorescent metalloproteinase substrates for cancer detection. Clin. Biochem., 44, 1434–1439.
11. Rao, V.H. et al. (2012) A positive feedback loop between HER2 and ADAM12 in human head and neck cancer cells increases migration and invasion. Oncogene, 31, 2888–2898.
12. Leyme, A. et al. (2012) Identification of ILK as a new partner of the ADAM12 disintegrin and metalloprotease in cell adhesion and survival. Mol. Biol. Cell, 23, 3461–3472.
13. Dulauroy, S. et al. (2012) Lineage tracing and genetic ablation of ADAM12(+) perivascular cells identify a major source of profibrotic cells during acute tissue injury. Nat. Med., 18, 1262–1270.
14. Lendeckel, U. et al. (2005) Increased expression of ADAM family members in human breast cancer and breast cancer cell lines. J. Cancer Res. Clin. Oncol., 131, 41–48.
15. Fröhlich, C. et al. (2013) ADAM12 is expressed in the tumour vasculature and mediates ectodomain shedding of several membrane-anchored endothelial proteins. Biochem. J., 452, 97–109.
16. Kveiborg, M. et al. (2005) A role for ADAM12 in breast tumor progression and stromal cell apoptosis. Cancer Res., 65, 4754–4761.
17. Le Pabic, H. et al. (2003) ADAM12 in human liver cancers: TGF-beta-regulated expression in stellate cells is associated with matrix remodeling. Hepatology, 37, 1056–1066.
18. Li, H. et al. (2013) Metalloproteinase-disintegrin ADAM12 is associated with a breast tumor-initiating cell phenotype. Breast Cancer Res. Treat., 139, 691–703.
19. Li, H. et al. (2012) An essential role of metalloprotease-disintegrin ADAM12 in triple-negative breast cancer. Breast Cancer Res. Treat., 135, 759–769.
20. Nariţa, D. et al. (2010) Molecular profiling of ADAM12 gene in breast cancers. Rom. J. Morphol. Embryol., 51, 669–676.
21. Narita, D. et al. (2011) ADAM12 and ADAM17 gene expression in laser-capture microdissected and non-microdissected breast tumors. Pathol. Oncol. Res., 17, 375–385.
22. Narita, D. et al. (2012) Increased expression of ADAM12 and ADAM17 genes in laser-capture microdissected breast cancers and correlations with clinical and pathological characteristics. Acta Histochem., 114, 131–139.
23. Uehara, E. et al. (2012) Upregulated expression of ADAM12 is associated with progression of oral squamous cell carcinoma. Int. J. Oncol., 40, 1414–1422.
24. Markowski, J. et al. (2009) Metal-proteinase ADAM12, kinesin 14 and checkpoint suppressor 1 as new molecular markers of laryngeal carcinoma. Eur. Arch. Otorhinolaryngol., 266, 1501–1507.
25. Carl-McGrath, S. et al. (2005) The disintegrin-metalloproteinases ADAM9, ADAM12, and ADAM15 are upregulated in gastric cancer. Int. J. Oncol., 26, 17–24.
26. Fröhlich, C. et al. (2006) Molecular profiling of ADAM12 in human bladder cancer. Clin. Cancer Res., 12, 7359–7368.
27. Mino, N. et al. (2009) A disintegrin and metalloprotease 12 (ADAM12) is a prognostic factor in resected pathological stage I lung adenocarcinoma. J. Surg. Oncol., 100, 267–272.
28. Kodama, T. et al. (2004) ADAM12 is selectively overexpressed in human glioblastomas and is associated with glioblastoma cell proliferation and shedding of heparin-binding epidermal growth factor. Am. J. Pathol., 165, 1743–1753.
29. Georges, S. et al. (2013) A Disintegrin And Metalloproteinase 12 produced by tumour cells accelerates osteosarcoma tumour progression and associated osteolysis. Eur. J. Cancer, 49, 2253–2263.

30. Sasaroli, D. et al. (2011) Novel surface targets and serum biomarkers from the ovarian cancer vasculature. Cancer Biol. Ther., 12, 169–180.
31. Cheon, D.J. et al. (2014) A collagen-remodeling gene signature regulated by TGF-β signaling is associated with metastasis and poor survival in serous ovarian cancer. Clin. Cancer Res., 20, 711–723.
32. Karlan, B.Y. et al. (2014) POSTN/TGFBI-associated stromal signature predicts poor prognosis in serous epithelial ovarian cancer. Gynecol. Oncol., 132, 334–342.
33. Diaz, E.S. et al. (2013) Obesity-associated adipokines correlate with survival in epithelial ovarian cancer. Gynecol. Oncol., 129, 353–357.
34. Li, A.J. et al. (2010) Serum low-density lipoprotein levels correlate with survival in advanced stage epithelial ovarian cancers. Gynecol. Oncol., 116, 78–81.
35. Cancer Genome Atlas Research Network (2011) Integrated genomic analyses of ovarian carcinoma. Nature, 474, 609–15.
36. Tothill, R.W. et al. (2008) Novel molecular subtypes of serous and endometrioid ovarian cancer linked to clinical outcome. Clin. Cancer Res., 14, 5198–5208.
37. Huang, R.Y. et al. (2013) An EMT spectrum defines an anoikis-resistant and spheroidogenic intermediate mesenchymal state that is sensitive to e-cadherin restoration by a src-kinase inhibitor, saracatinib (AZD0530). Cell Death Dis., 4, e915.
38. Roy, R. et al. (2004) ADAM 12 cleaves extracellular matrix proteins and correlates with cancer status and stage. J. Biol. Chem., 279, 51323–51330.
39. Matsuo, K. et al. (2012) Significance of lymphovascular space invasion in epithelial ovarian cancer. Cancer Med., 1, 156–164.
40. Chang, S.J. et al. (2012) Impact of complete cytoreduction leaving no gross residual disease associated with radical cytoreductive surgical procedures on survival in advanced ovarian cancer. Ann. Surg. Oncol., 19, 4059–4067.
41. Vergote, I. et al. (2010) Neoadjuvant chemotherapy or primary surgery in stage IIIC or IV ovarian cancer. N. Engl. J. Med., 363, 943–953.
42. Prat, A. et al. (2013) Characterization of cell lines derived from breast cancers and normal mammary tissues for the study of the intrinsic molecular subtypes. Breast Cancer Res. Treat., 142, 237–255.
43. Konecny, G.E. et al. (2014) Prognostic and therapeutic relevance of molecular subtypes in high-grade serous ovarian cancer. J. Natl. Cancer Inst., 106(10). pii: dju249. doi:10.1093/jnci/dju249.
44. Zhang, W. et al. (2013) Integrating genomic, epigenomic, and transcriptomic features reveals modular signatures underlying poor prognosis in ovarian cancer. Cell Rep., 4, 542–553.
45. Egeblad, M. et al. (2010) Tumors as organs: complex tissues that interface with the entire organism. Dev. Cell, 18, 884–901.
46. Ramdas, V. et al. (2013) Canonical transforming growth factor-β signaling regulates disintegrin metalloprotease expression in experimental renal fibrosis via miR-29. Am. J. Pathol., 183, 1885–1896.
47. Ray, A. et al. (2010) Transforming growth factor-beta1-mediated activation of NF-kappaB contributes to enhanced ADAM-12 expression in mammary carcinoma cells. Mol. Cancer Res., 8, 1261–1270.
48. Iba, K. et al. (1999) Cysteine-rich domain of human ADAM 12 (meltrin alpha) supports tumor cell adhesion. Am. J. Pathol., 154, 1489–1501.
49. Bourd-Boittin, K. et al. (2008) RACK1, a new ADAM12 interacting protein. Contribution to liver fibrogenesis. J. Biol. Chem., 283, 26000–26009.
50. Huppertz, B. et al. (2006) Trophoblast fusion: fusogenic proteins, syncytins and ADAMs, and other prerequisites for syncytial fusion. Micron, 37, 509–517.